LPR/NB RI/FS MODELING PROGRAM

STATUS OF THE CPG'S SEDIMENT TRANSPORT MODEL

Prepared for:

Put client's name or a logo

Rev No	A	–	–	–	–
Issue Purpose	**Client Approval**				
Date					
By					
Checked					
Approved					

Prepared by:

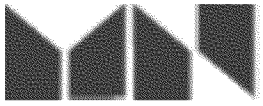

TABLE OF CONTENTS

LIST OF FIGURES

LIST OF TABLES

1.0 INTRODUCTION

The ongoing RI/FS of the Lower Passaic River Study Area (LPRSA) being conducted by the Cooperating Parties Group (CPG) includes the development of a Sediment Transport (ST) model of the Lower Passaic River (LPR) and Newark Bay (NB). The CPG's model development and calibration process follows the approach outlined in the LPR and NB Modeling Work Plan (MWP) documents (HydroQual 2006a, and HydroQual 2006b). The model framework is identical to the one used by Region 2 for their revised Remedial Investigation-Focused Feasibility Study and involves an implementation of the SEDZLJ ST algorithm developed by Jones and Lick (2001) within the computational framework of the ECOM hydrodynamic model. During the course of its application to the LPR and NB, SEDZLJ has been further developed by Region 2 to include a bed consolidation model developed by Sanford (2008). The combined hydrodynamic and ST modeling framework is referred to as the ECOM-SEDZLJS model.

The model development and calibration reported in this memorandum are based on model code and input files received from Region 2 in November, 2011 and which were modified in several aspects as described subsequently in this document. Region 2 has been periodically updated on the CPG's ST modeling efforts through presentations at the Semi-Annual Modeling Meeting and Modeling Collaboration Meeting forums. Although considerable progress has been made with regard to the model calibration and performance within the LPR, it should be noted that additional work remains to be done, most notably in the calibration and performance within NB, and to the extent that ongoing development and calibration of the contaminant fate and transport model necessitates further refinement of the ST model. Therefore, the model calibration parameters and results are presented as a work-in-progress subject to further review and revision, rather than a final work product.

During the Modeling Collaboration Meeting between various Region 2 and CPG representatives on September 25 2012, Region 2 requested the CPG provide a memorandum describing the status of the CPG's ST model development and its application to the LPR and NB. The goal of this document is to fulfill Region 2's request. The remainder of this memorandum describes the CPG's system understanding as it pertains to sediment transport, the ST model setup, calibration and results, and future tasks.

2.0 SEDIMENT TRANSPORT SYSTEM UNDERSTANDING

The development and application of a model for a given site usually involves an assessment of the major processes relevant to the problem to be addressed with the model. In the case of the ST model described in this document, this assessment has been carried out using a number of datasets and tools, in particular:

- The hydrodynamic model developed by Region 2 (HydroQual 2008),
- A high-resolution hydrodynamic model developed by the CPG,
- Data collected by Sommerfield and Chant (2010) as part of their NB monitoring study,
- Data from the Fall 2009 and Spring 2010 Physical Water Column Monitoring (PWCM[1]) program
- Data from the 1949 post-dredge bathymetric survey and 1966 bathymetric conditions survey, and
- Data from the 2007, 2008, 2010, 2011, and 2012 multi-beam bathymetric surveys.

The analyses allow for an empirical understanding of sediment transport processes in the LPRSA and NBSA and provide calibration targets for the ST model. This system understanding of sediment transport processes is more complete for the LPRSA than for the NBSA, and therefore the analyses and model results reported in this document are restricted to the LPRSA. This section describes the spatial domain, and the results of analyses to understand the major transport processes relevant to sediment transport in the LPRSA.

2.1 Spatial Domain

The ST model domain includes the 17.4-mile tidal stretch of the LPR extending from Dundee Dam to the mouth at Newark Bay, the Hackensack River (including the Meadowlands wetlands) from Oradell Dam to its mouth at Newark Bay, Newark Bay, and the tidal inlets to Newark Bay, namely the Arthur Kill extending to Raritan Bay and the Kill van Kull extending to upper New York bay (Figure 1). In addition to the discharge and suspended sediments entering from the freshwater and open boundaries listed above, several minor tributaries (Second River, Third River, Saddle River, and McDonald Brook), combined sewer outfalls, and storm-water outfalls also discharge into the LPR/NB domain.

[1] The Fall 2009 PWCM suspended sediment data referenced in this document includes the estimates of suspended sediment concentrations from acoustic back-scatter (ABS) estimates calculated from the echo intensity measurements made by the *in situ* ADCP moorings. These estimates were first derived by EPA in 2010, and updated in 2011 following a revision to the ABS estimates as well as a combined analysis of the ABS to suspended sediment correlation in the Fall 2009 and the Spring 2010 PWCM data. The revised estimates are under review and need to be incorporated into the various analyses. Therefore, the data analyses presented in this document are restricted to the Fall 2009 PWCM survey data, and using the suspended sediment estimates derived in 2010.

Historically, both the LPR and NB were extensively used for shipping and dredged to depths well below the pre-industrial conditions (Chant et al. 2011). The reach above RM 6.8 in the LPR was last dredged in 1932 and between RM 6.8 – 2.5 in 1949. The navigation channel in the lower reach (RM 0 – 1.5), however, was dredged as recently as 1983. Following the decline of shipping activities in the LPR, the navigation channel was not maintained and has subsequently filled in with sediment. Current dredging activities are limited to isolated berthing facilities at the mouth of LPR, along with maintenance and capital dredging in the lower half of NB and the Kills.

The model grid used for representing this network of inter-connected water bodies is shown in Figure 1; it derives from the grid developed by Region 2 for the hydrodynamic model (HydroQual 2008). Within the LPR, the average grid size is 40 m wide and 180 m long, with the river typically represented with 4 cells across (decreasing to 3 cells above RM 4.4, and 2 cells above RM 15.7), and the former navigation channel represented by 1-2 cells. Lateral bathymetric gradients in the LPR are often steep, ranging from about 25 ft. below NGVD in the deepest parts of the former navigation channel, to a few feet below NGVD on the shallows, to NGVD in the intertidal areas. With only 4 cells to represent this wide range of depths, the hydrodynamic model cannot reproduce the flow patterns, velocities, and shear stresses in great detail, especially in the vicinity of features such as river bends, and in-water structures such as bridge abutments. Furthermore, several of the erosional and depositional features that have been observed in the analysis of the recent multi-beam bathymetries are sub-grid scale features compared to the size of the individual model grid cells. For these reasons, the sediment transport model cannot be expected to fully resolve the spatial heterogeneity of the features and processes observed in the data. In order to develop a better understanding of the shear stress regime, a high resolution hydrodynamic model was developed and applied as described in the following section.

2.2 High Resolution Hydrodynamic Model

The high-resolution hydrodynamic model was developed in order to better quantify the distribution of velocities and shear stresses within the LPR. The increased resolution was necessary to resolve features and processes such as secondary flow in river bends, cross-channel variability in flow patterns, and the presence of in-river structures such as bridge abutments. While the spatial extent of the high resolution hydrodynamic model was maintained the same as the ST model, the resolution was increased by roughly 4-5 and 2-3 times in the longitudinal and lateral directions, respectively, in the LPR (average grid size is 18 m wide and 42 m long). The model bathymetry within the LPR was based on the USACE single beam survey conducted in 2004.

The model was calibrated to the hydrodynamic data (water levels, velocities, and salinity) collected by Rutgers University in 2004 (dataset also used for the calibration of the LPR/NB hydrodynamic model; HydroQual 2008) which covered flows ranging from a few 100s cfs to 3000 cfs. The trade-off for higher resolution is increased simulation times, and consequently the high resolution model could not be applied for a long-term

simulation. Rather, the calibrated model was applied to a series of constant river discharges covering typical spring-neap tidal cycles to obtain shear stress maps under varying conditions. These maps also formed the basis of a look-up table of predicted shear stresses as a function of tide and discharge, which was used to estimate shear stresses for the high-resolution grid over a 20-year period beginning in 1989. These maps were used for an assessment of the spatial and temporal distribution of shear stresses and to inform the system understanding analyses.

Note that although a constant bathymetry (2004) was used in the high resolution model, changes in bathymetry are small compared to the overall water depth, even after an extreme event such as Hurricane Irene.. Hence, yearly variations in bathymetry will not strongly affect the overall flow patterns, though locally flow velocities and bed shear stresses may be affected.

2.3 Transport Processes

Hydrodynamic transport processes within the LPR are controlled by the tides, freshwater discharge, and estuarine circulation (Chant et al. 2011). Semi-diurnal tides entering Newark Bay through the Kill van Kull and Arthur Kill propagate through NB to LPR and to the head-of-tide at Dundee Dam. Measurements along the longitudinal axis of the LPR and NB show a pronounced longitudinal gradient in salinity, with relatively high salinity in NB and decreasing with distance up-estuary into the LPR. Because of the density differences between saline and freshwater, the freshwater discharge from Dundee Dam tends to flow on top, subject to turbulent mixing with the denser salt water entering from the Kills resulting in a partially mixed water column within the LPR. The longitudinal pressure gradient induced by the longitudinal salinity gradient generates a net near-bed flow up-estuary, and a net down-estuary flow in the upper half of the water column – this circulation is known as the estuarine or gravitational circulation, and the mass flow induced is balanced by vertical mixing and entrainment processes.

The zone of transition from freshwater to brackish, i.e. the salt front, is also typically associated with the Estuarine Turbidity Maximum (ETM), an area of relatively high suspended sediment concentrations and also sediment deposition (Dyer 1997). The salt front also represents the upstream-most extent of the estuarine circulation process, and therefore the upstream-most extent of the suspended solids originating from the down-estuarine portion of the river. Hydrodynamic and sediment transport during normal tidal and discharge conditions in the estuarine portion of the LPR are also characterized by tidal asymmetry, with higher velocities and suspended sediment concentrations during flood than on ebb. The combination of estuarine circulation and tidal asymmetry results in suspended solids fluxes directed up-estuary within the salt wedge and directed down-estuary in the freshwater section. Given the bi-directional nature of the suspended sediment fluxes as a function of the location of the salt front, the exchange between the LPR and NB becomes an important element of the sediment transport within the LPR. Each of these processes is further examined in the following sections.

2.3.1 Salt Front

The location of the salt front varies spatially and temporally. For discussion purposes in this document, the salt front is located at the point of 2 ppt salinity at the bottom of the water column. During normal tidal and discharge conditions, the salt front is within the LPR, at a location dependent on the freshwater discharge, inter-tidal timing (spring/neap), intra-tidal timing (flood/ebb), and offshore set-up/set-down events.

Figure 2 shows the location of the salt-front as a function of the river discharge, with the salt-front location computed using a hydrodynamic simulation from water year 1995 through 2004 using the model developed by Region 2 (HydroQual 2008). The time-series of computed salt front locations was low-pass filtered in order to extract only the response to discharge events. The results indicate that the salt-front is situated up-estuary of RM 5 when discharge at Dundee Dam is below the annual average of 1,200 cfs (HydroQual 2006a; 1,140 cfs at Little Falls with drainage-area proration to calculate discharge at Dundee Dam). The salt-front location is pushed down-estuary with increasing flow and at 2,000 cfs it is found on average near RM 3. During a 1-year return flow of about 6,000 cfs, the salt front is pushed below RM 2, while a 5-year return flow of about 10,000 cfs pushes the salt front below RM 1, where the river widens rapidly. The location of the salt front is also a function of the tidal cycle, with tidal excursion lengths on the order of 2.5 to 4.5 miles from low to high tide.

2.3.2 Estuarine Turbidity Maximum

Several data sources indicate the presence of a well-defined ETM associated with the salt front within the LPR and NB (Chant et al. 2011; Mathew et al. 2011). Shipboard measurements of salinity and suspended sediment concentrations along longitudinal transects of the LPR and NB (Chant et al. 2011) as well as analysis of the suspended sediment concentrations measured during the Fall PWCM (Mathew et al. 2011) show both the presence of the ETM in the vicinity of the salt front, as well as the dynamic nature of the ETM location and concentrations. Figure 3 shows the salinity contours, and suspended sediment concentrations measured during two different discharge conditions, the upper panel during low-flow conditions (June 23, 2005 with discharge of 250 cfs at Little Falls), and the lower panel during high-flow conditions (16,000 cfs storm-event on March 16, 2010; both datasets measured by Dr. Bob Chant of the Institute of Marine and Coastal Science, Rutgers University). Both transects show higher suspended sediment concentrations in the vicinity of the salt front than at locations up-estuary or down-estuary of it. During the low-flow survey both the salt front and the ETM are located at RM 7, with depth-average suspended sediment concentrations of ~100 mg/L within the ETM. In contrast, during the high-flow survey, the salt front and the ETM are pushed to RM 0 with much higher depth-average suspended sediment concentrations of ~250 mg/L, a likely consequence of the higher river discharge. Around the slack phase of the tide, as flow velocities and shear stresses decrease, suspended sediments deposit from the water column, with the highest deposition fluxes expected within the ETM.

2.3.3 Tidal Variability

Under normal tidal and discharge conditions, suspended solids concentrations are affected by tidal asymmetry, intra-tidal variability, and inter-tidal variability driven by similar fluctuations in velocities. As shown in Figure 4, under normal tidal and discharge conditions, suspended solids concentrations are higher during flood than on ebb for all locations within the salt wedge (this is the result of a process known as internal tidal asymmetry.) In combination with a similar asymmetry in velocities, this represents a net up-estuary flux (per tidal cycle) of suspended sediments at all locations within the salt wedge, a process termed as tidal pumping. In contrast, the freshwater station (RM 13.5) shows very little variability within the tidal cycle.

The suspended solids data also show systematic patterns with velocity, with concentrations increasing as velocity increases, reaching a maximum around the time of maximum velocity and decreasing thereafter to a minimum around slack water. This general pattern is true of both ebb and flood tides for all locations within the salt wedge. This intra-tidal variability is indicative of a pool of easily erodible sediment, termed a fluff layer, deposited on the bed during slack water and resuspended during the following flood or ebb tide (Maa et al. 1998, Van Kessel et al. 2007, El Ganaoui et al. 2004, Wang 2003). Using the range in suspended sediment concentrations within the flood tide of ~50 to ~150 mg/L at the various locations within the salt wedge, with average water depth of 5 m, and assuming a low dry density of 100 Kg/m^3 results in estimated fluff layer thickness ranging from 2 mm to 7 mm.

The suspended solids data also exhibit inter-tidal variability as shown in Figures 5 and 6, with higher suspended sediment concentrations during spring tides (tidal range of ~2m) than during neap tides (tidal range of ~1m) at all locations within the predominantly estuarine portions of the river (RMs 1.4, 4.2, and 6.7 during this deployment.) Review of the suspended solids time-series at RM 1.4 (Figure 5 second panel from top, and Figure 6) suggests that the bed-water exchange are dominated by the fluff layer dynamics up to discharge of ~2,000 cfs at Dundee Dam, with suspended solids concentrations increasing as discharge increases beyond ~2,000 cfs. Comparing to the annual average discharge of 1,200 cfs at Dundee Dam suggests that fluff layer dynamics dominate sediment transport within the LPR the majority of the time. The response at discharge higher than ~2,000 cfs may indicate a combination of higher suspended solids loads from Dundee Dam and/or erosion of the more consolidated sediments underlying the fluff layer.

2.3.4 Tidal Pumping

The direction and magnitude of the net daily suspended sediment fluxes computed using paired measurements of suspended sediment (from acoustic backscatter measurements) and velocities from the moored ADCPs during the Fall PWCM are shown in Figure 7 as a function of the measured daily discharge at Dundee Dam. Both suspended sediment and velocity profiles measured by the ADCPs have been extrapolated to the unmeasured depths at the near-bottom and the near-surface of the water column. The ADCP

measured vertical structure of the velocity and suspended sediment concentrations have not been extrapolated across the width of the river; rather the fluxes are expressed per unit width of the river. In addition to the Fall PWCM data, data collected at RM 1.4 by Sommerfield and Chant (2010) as part of their NB study have also been analyzed and are presented in Figure 7. As expected given the trends in the suspended sediment and velocity noted previously, the net solids fluxes show the integrated effects of the tides, estuarine circulation, and freshwater discharge. At all the locations within the predominantly estuarine sections of the river (RMs 1.4, 4.2, and 6.7 during this deployment), below a certain discharge threshold solids fluxes are directed up-estuary. Only at the freshwater station (RM 13.5) is the net solids flux consistently directed down-estuary. The discharge associated with the inflection in the direction of solids fluxes decreases with distance up-estuary; the point of inflection at any given location is also consistent with the discharge associated with the passage of the salt front past that location (shown in Figure 2).

It is important to realize that the three important processes, i.e. estuarine circulation, tidal asymmetry (pumping) and river-induced flushing induce a convergence of fine sediment transport around the estuarine turbidity maximum for fine sediments originating from both up-estuary (Dundee Dam) and down-estuary (Newark Bay) and all other sediment inputs.

2.3.5 Exchange with Newark Bay

Given the availability of long-term monitoring data, for purposes of this document, the exchange between the LPR and NB is characterized at RM 1.4 in the LPR. It is anticipated that the exchange between the LPR and NB may be more accurately resolved at RM 0.9 following the development of the system understanding of sediment transport in NB and the development of the ST model for NB. Down-estuary of RM 0.9, the river widens rapidly. Because of the tidal pumping and estuarine circulation processes described previously, the exchange between the LPR and NB is an important element of the solids balance for the LPR. Both the datasets presented in Figure 7 show that at RM 1.4, suspended sediment fluxes are directed up-estuary up to ~1500 cfs i.e., infilling regimes, with net export of suspended sediments from the LPR at higher discharges, i.e. exporting regimes.

2.3.6 Infilling

In addition to suspended sediment data, several recent and historic datasets show evidence of infilling within the LPR. Historic data sources include the 1949 post-dredge bathymetry between RM 2.5 and RM 6.8, the 1966 bathymetric survey[2] between RM 2.3 and RM 7.8, and the 1983 post-dredge bathymetry between RM 1.5 and RM 0. Recent datasets include the 2007, 2008, 2010, 2011 and 2012 multi-beam bathymetries.

[2] The 1966 conditions bathymetry is generally consistent with the depth of the cesium peak measured in the CLRC (AECOM 2010) and Tierra (CLH 1995) coring programs

Comparison of these historic bathymetries to the current conditions (for discussion purposes, 2010) shows accumulations of as much as 15 ft. within the dredged channel. Comparison of the recent multi-beam bathymetries also shows infilling within the LPR during low-flow periods (described in further detail in the following section). The Environmental Dredging Pilot Study (EDPS; MPI 2007a) also showed rapid infilling of the excavation pit following the completion of dredging, at rates up to 3 mm/day (using a Volume of Cut method to analyze the infill rate).

2.3.7 Current Morphological Behavior

Comparison of the various recent multi-beam bathymetries (2007, 2008, 2010, 2011 and 2012) within the LPR show morphological behavior that is dependent on the hydrographic conditions. For instance, the 2010 and the 2011 surveys which followed a 16,000 cfs event (25-year event; MPI 2007b) and Hurricane Irene (24,000 cfs; 100-year event; MPI 2007b), respectively, show most notably erosion in the vicinity of bridge abutments or features such as river bends, and deposition downstream of RM 1 where the river widens and shear stresses decrease. However, during low-flow periods such as between the 2007 and 2008, and the 2011 and 2012 surveys, areas that experience erosion during high-flow periods show deposition, whereas areas at the mouth of the river with deposition during high-flow periods show erosion during low flow periods. Examination of the shear stress maps generated from the high resolution hydrodynamic model suggests that the erosion at the mouth of the river during low-flow periods may be for reasons other than normal tidal hydrodynamics. In particular, ongoing shipping activities within the LPR can have a potential impact on shear stresses and resuspension and will be investigated in future analyses. The analysis of the bathymetric surveys also suggests that the LPR may be approaching its post-dredge equilibrium condition, although the bathymetric features at any given point in time may reflect the preceding hydrographic conditions (infilling or erosional).

2.4 System Understanding Summary

The data and analyses reported herein inform the relationship between sediment transport and various forcings such as freshwater discharge from Dundee Dam and the intra- and inter-tidal fluctuations. The data also inform on processes such as the location of the ETM and the exchange between the LPR and NB under various flow and tidal conditions. At discharge less than ~1,500 cfs, because of tidal pumping and estuarine circulation, the LPR can be considered to be net infilling with suspended solids transported down-estuary from Dundee Dam and up-estuary from NB. Net export from the LPR only occurs at discharge greater than ~1,500 cfs. On average, the LPR is more or less in morphodynamic equilibrium, though variations around this equilibrium may occur in response to a series of river floods, or prolonged periods with average or below-average flows.

These analyses, in conjunction with other data sources, provide necessary information to parameterize and calibrate the sediment transport model within the LPR and the exchange

between the LPR and NB. In particular, processes that can be considered key to reproducing the sediment dynamics of the LPR include the location and suspended sediment concentrations within the ETM, the intra- and inter-tidal variability in suspended sediment concentrations, tidal pumping, and infilling. Infilling is an especially important process because of the presence of alternating (dependent on the hydrograph) erosional and depositional features in the river. In addition, the remedial alternatives to be considered as part of the RI/FS process could include dredging to the Federally-mandated navigation channel depths at selected locations within the LPR. In such a scenario, the model's ability to reproduce infilling will be essential in simulating the evolution of the post-dredge morphology.

3.0 MODEL SETUP AND DEVELOPMENT

The model setup, development, and calibration are inherently an iterative process. Application of the model initially focused separately on high and low-flow conditions, i.e., exporting and importing regimes. For instance, the low-flow application involved a model of only the LPR forced with the measured tides and suspended sediment data at RM 1.4 during the Fall PWCM, whereas the high-flow application was only focused on reproducing the suspended solids data measured during the 16,000 cfs event on March 16, 2010. This was followed by a combined application to both high and low-flow conditions as well as to long-term periods. Only the resulting model framework and parameterization are presented in this document along with a explanation of the rationale for the model parameterization and code modifications.

3.1 Time Periods Modeled

The time-periods chosen for the ST model application were intended to bracket the periods with the greatest amount of data for model-data comparisons. Accordingly, these periods correspond to calendar years 2007, 2008, 2009, 2010, and 2011, covering the recent multi-beam bathymetry datasets, the 2009 Fall and 2010 Spring PWCM data, the data from the 16,000 cfs event on March 16, 2010, and the 2008-09 NB deployment by Sommerfield and Chant (2010). In addition, given the objective of supporting the long-term calibration and application of the contaminant fate and transport model, the ST model was also applied over a long-term simulation from 1995 to 2011.

3.2 Model Inputs

The ST model requires a number of inputs including,

- The size and number of particle classes
- Mass fraction of each particle class in the sediment bed per model cell
- Sediment bed dry density per model cell
- Boundary conditions for suspended sediments
- Erosion properties
    - Erosion rate as a function of shear stress
    - Critical shear stress for erosion
- Settling velocities for each particle class

3.2.1 Particle Size Classes and Distribution

The trends in suspended solids concentrations within the tidal cycle presented in Figure 4 suggest the presence of suspended solids with very different settling velocities within the LPR – a solids class with higher settling velocity within the estuarine section and a slower settling class within the freshwater section. The slower settling class is indicative

of fine sediments associated with the wash load from Dundee Dam and the faster settling class indicative of solids originating from marine or estuarine sources and transported up-estuary into the LPR within the salt wedge. The faster settling particles in the down-estuary part of the river are the result of spatial segregation and flocculation in the saline environment. The sediment classes in motion during such normal tidal and discharge conditions are expected to be fine sediments, (particle size <63 um) given the relatively muddy sediment substrate within the LPR, especially in the lower 8 miles. Therefore two solids classes are used to represent the fines within the LPR and NB, with size classes corresponding to <4 um (clays), and 4-63 um (silts). In contrast to the lower reaches of the LPR, the areas above RM 8 are predominantly sandy, especially within the former navigation channel. In addition to the core data, the bed forms and sand waves observed within the upper reach in some of the recent multi-beam bathymetry datasets suggest a sandy substrate with non-cohesive transport during storm events. In order to achieve a reasonable depiction of non-cohesive transport processes such as bed armoring, three non-cohesive grain size classes were chosen corresponding to 63-450 um (fine sand), 450-2000 um (medium sand), and >2000 um (coarse sand).

The sediment grain size distribution data from core samples were used to evaluate the diameter associated with each of the five particle size classes and the relative distribution of these classes over the LPR and NB model domain. Data from several sampling programs listed below were used in this analysis:

- 2008 CPG Low-res coring program
- 2007 Newark Bay RIWP Phase 2 SI
- 2005 Newark Bay RIWP Phase 1 SI
- 2000 Spring RI-ESP Sampling Program
- 1999/2000 Minish Park Monitoring Program
- 1999 Late Summer/Early Fall RI-ESP Sampling Program
- 1999 Preliminary Toxicity Identification Evaluation Study

The particle size for each class was assigned as the median of the class size computed for the individual core samples and is shown in Table 1.

The sediment mass fraction within each of the size classes was also evaluated using the datasets listed above and is shown in Figure 8 for the data in the top 6" of the bed. Laterally within the LPR, the main feature seen is a distinction between the data inside and outside the former navigation channel, with coarser sediments within the former navigation channel and finer sediments outside. The main longitudinal feature is a coarsening of the sediments with distance up-estuary within the former navigation channel. These features were included within the initial conditions for the ST model by developing averages separately for the data inside and outside the former navigation channel and over distinct longitudinal reaches (RM 0-2, RM 2-4, RM 4-6, RM 6-8, RM 8-13, and RM >13). The model grid cells within each spatial reach were assigned to the averages derived for inside or outside the channel in that reach depending on the spatial overlay of the model grid and the navigation channel. This process was followed for the

depth intervals 0'-0.5', 0.5'-1.5', 1.5-2.5', 2.5-3.5', and 3.5'-5.5' depth intervals, following the core segmentation in the CLRC program (AECOM 2010).

Table 1. Effective Diameters for Particle Size Classes in the LPR and NB ST Model Application

Size Class	Effective Diameter (um)
Clays(<4 um)	2
Silts (4-63 um)	17
Fine Sand (63-430 um)	140
Medium Sand (430-2000 um)	670
Coarse Sand (>2000 um)	3100

3.2.2 Dry Density

The sediment dry densities were determined from solids content measurements from core samples (from the datasets listed previously for grain size distribution) and assuming particle specific gravity of 2.65. The data were averaged over the same lateral and longitudinal spatial resolution as the grain size distribution data described above. The values for the individual core samples as well as the averages computed for the model inputs are shown in Figure 9 and show similarities with the grain size distribution. As expected given the coarser sediments within the former navigation channel in the upper reaches of the LPR, dry density is higher in these sections than areas outside the former channel. These dry density averages were assigned to the individual model cells using the same procedure described for the grain size distribution above.

3.2.3 Boundary Conditions

Rating curves for the inflowing sediment concentrations at the open boundaries were developed based on analysis of data collected by Sommerfield and Chant (2010). The measured suspended solids concentrations at Kill van Kull showed correlations with flow velocity and tidal range, and also a seasonal dependency between winter/spring and summer/fall which are typically the local high and low precipitation months, respectively. All of these factors were incorporated into the rating curve for sediment load at the Kill van Kull, which was prescribed by fitting the following curve to the data:

$$\text{Suspended Sediment Load} = a * U^b * TR^c * SF$$

where U = velocity in m/s, TR = tidal range in m, Load in $g/m^2/s$, a = proportionality constant, SF = seasonality factor (applicable during the months of December to April), and b and c are parameters fit to the data. Distinct trends in concentration were observed

within the accelerating and decelerating phases of the flood tide, which suggested the use of separate functions for these phases. Table 2 lists the rating curve coefficients for each of the sigma levels (water column layers) used to prescribe the solids boundary condition at the Kill van Kull.

Table 2. Rating curve functions for the solids boundary condition at Kill van Kull

Sigma Level	a	b	c	SF
Case: Accelerating Flood Tide				
10	110.94	1.91	-0.05	1.38
9	68.38	1.84	0.06	1.31
8	43.17	1.93	0.14	1.26
7	23.68	1.81	0.69	1
6	14.05	1.85	1.16	1
5	12.01	1.90	1.15	1
1 to 4	13.76	1.88	0.65	1
Case: Decelerating Flood Tide				
10	66.93	1.37	0.55	1.38
9	51.11	1.40	0.67	1.31
8	32.32	1.33	0.86	1.26
7	22.32	1.27	1.27	1
6	15.84	1.27	1.62	1
5	13.44	1.28	1.70	1
1 to 4	13.13	1.32	1.35	1

In contrast to the Kill van Kull, suspended solids at the Arthur Kill did not suggest any relationships with the flow velocity, and only a linear relationship with the tidal range could be positively identified and fit using a function of the form:

$$\text{Suspended Sediment Concentration} = m * TR + c$$

where concentration is in mg/L, and TR = tidal range in m. Table 3 lists the rating curve coefficients for each of the sigma levels (water column layers) used to prescribe the solids boundary condition at the Arthur Kill.

These rating curves were used to develop solids boundary conditions time-series using the water levels and velocities calculated by the hydrodynamic model for any given period. The sediment inputs at these open boundaries were assigned to the silt (4-63 um) size class within the model.

For the inflow boundaries at Dundee dam, river tributaries, flow-dependent rating curves developed by Region 2 were used to prescribe depth-average sediment inputs to the model. The regressions were based on a log-curve fit to the respective river/tributary discharges, with different relationships for discharges below and above a certain threshold. Under low to average flow conditions, all the sediment inputs were assigned to the clay (< 4um) size class, with a small proportion of fine sands also included when flows exceed a given threshold. Solids inputs from the CSO and SWO boundaries are also identical to those developed by Region 2 for their revised Remedial Investigation-Focused Feasibility Study.

Table 3. Rating curve functions for the solids boundary condition at Arthur Kill

Sigma Level	m	c
10	7.09	6.55
9	4.42	5.07
8	3.04	3.97
7	2.78	3.32
6	2.12	3.28
5	1.55	3.19
4	1.46	2.84
3	1.82	2.33
2	2.52	1.77
1	3.41	1.19

3.2.4 Erosion Properties

The process of model setup and calibration was an iterative process and included a number of modifications to the original ECOM-SEDZLJS framework. Although described in additional detail in the following section, one such modification involved the vertical discretization of erosion properties within the sediment bed. Conceptually, the original model framework was modified to include a fluff layer overlying more consolidated bed layers. In other words, a low strength (or easily erodible) fluff layer overlying a stronger or less erodible layer (strength in this context is meant to refer to the critical shear stress for erosion). The erosion properties (the critical shear stress for

erosion and the erosion rate) of both layers were derived from site-specific data and are described in the following sections.

Fluff Layer

Erosion properties for the fluff layer were derived from an analysis of suspended sediment data from the Fall PWCM. Review of the Fall PWCM data showed some consistent patterns – during all periods when the salt front and therefore the ETM were located above RM 4.2, suspended solids concentrations at RM 4.2 during the flood tide was generally higher than at RM 1.4 (as seen in Figure 4). The concentrations were also noted to be positively correlated with the flow velocity within the tidal cycle. This increase in concentrations was considered to be associated with erosion between RM 1.4 and 4.2 during the given flood tide. Considering only the period of accelerating velocity on the flood tide (which is also the period of increasing suspended solids concentrations), the increase in concentrations from RM 1.4 to 4.2 likely represents gross erosion rather than net erosion. However, since the analysis uses suspended solids measurements rather than direct measurements of erosion, the analysis is presented in terms of the entrainment process rather than the erosion process. The increase in concentrations in time was converted to an entrainment rate and related to the velocity and shear stress regime. Considering only the data during normal discharge and tidal conditions when fluff layer dynamics are considered to dominate sediment transport within the LPR, this entrainment represents erosion from the fluff layer and can therefore inform the erosion properties of the fluff layer.

The Fall PWCM included continuous (every 12 minutes) measurements of velocity, salinity, water depth, and the suspended solids concentration profile at RM 4.2 amongst other locations. The increase in depth-average suspended solids concentration from one measurement to the next was converted to an entrainment rate over that time-interval using the water depth and an assumed dry density of 500 Kg/m^3 for the fluff layer. Although the actual densities of the fluff layer are likely to be much lower than the value assumed for this calculation, since the objective of this calculation was to develop an input for the model, the assumed value approximates the dry density of the surficial sediments in the ST model. The resulting entrainment rate was paired with the model predicted skin friction along the thalweg between RM 4.2 and 1.4 over that time period. The entrainment rate calculation was restricted to the period of minimum to maximum suspended solids concentration at RM 4.2 during the flood tide, only for periods not affected by advection from RM 1.4 (neglecting dispersion), and for periods in the Fall PWCM when the salt front and therefore ETM are located above RM 4.2 (Oct. 11–24, 2009 and Nov. 21–28, 2009).

The paired entrainment rate and shear stress are shown in Figure 10. Since the entrainment rates were calculated from high-frequency water column suspended solids measurements, they are susceptible to variability in the suspended solids concentrations. However, the variability (as seen in the range of entrainment rates as well as negative entrainment rates) is restricted to a relatively small subset of the entire dataset and is

more pronounced at the lower shear stresses (expected around slack water) when suspended solids concentrations are relatively low compared to other periods within the accelerating flood tide. The entrainment rate data were also binned over shear stress intervals and used to develop a functional relationship similar to the Sedflume erosion rate formulation. The relationship is approximately linear (n=1.07), with binned erosion rates ranging from ~$2x10^{-6}$ to ~$2x10^{-5}$ cm/s over the entire range of normal tidal shear stresses. Another important erosion property apparent from Figure 10 is the threshold for resuspension or the critical shear stress for erosion; entrainment is noted to occur only at shear stress greater than 0.5 dynes/cm^2 which suggests the critical shear stress for the fluff layer within the LPR/NB ST model framework. This critical shear stress is also comparable to measurements for the fluff layer at other sites (0.5 dynes/cm^2 reported by Wang 2003; 0.25-0.5 dynes/cm^2 reported by El Ganaoui et al. 2004; 0.5 dynes/cm^2 reported by Maa et al. 1998). The erosion rates ranging from ~$2x10^{-6}$ to ~$2x10^{-5}$ cm/s over the range of normal tidal conditions also overlap with reported values for other sites (constant 10^{-6} cm/s reported by Wang et al. 2003; 10^{-7} – $8x10^{-6}$ cm/s reported by El Ganaoui et al. 2004 over the same shear stress range). The results of the entrainment rate analysis were used to define the erosion properties for the fluff layer in the LPR/NB ST model – the critical shear stress for erosion was defined as 0.5 dynes/cm^2 and the erosion rate (in cm/s) was defined as a linear function of the shear stress with coefficient $5x10^{-6}$. The fluff layer thickness is set to 0.5 mm, based on the value estimated from the PWCM data (using dry density of 500 Kg/m^3, a value consistent with model definition for unconsolidated sediments).

Parent Layers

The parent layers in ECOM-SEDZLJS refer to the stack of consolidated sediment layers initialized in the model. Erosion properties for these layers were defined using data collected during the LPR Sedflume program (Borrowman et al 2006). Data from the LPR Sedflume core tests were analyzed for the dependency between erosion rate and shear stress. A function of the form $E = A\tau^n$ (where E=erosion rate in cm/s, τ=shear stress in Pa, and parameters A and n are empirically determined from the data) was fit to each of the shear stress sequences run through the Sedflume device for each core. The resulting functions were used to calculate the critical shear stress for erosion, calculated as the shear stress corresponding to erosion rate of 10^{-4} cm/s for each shear stress sequence run with each of the Sedflume cores; this is a relatively standard approach in the analysis of Sedflume erosion data.

The resulting erosion properties were analyzed for vertical and spatial heterogeneity. In general, the individual cores showed erodibility (as indicated by both erosion rate and the critical shear stress for erosion) decreasing with depth, a qualitatively reasonable expectation given that sediments at depth would be more consolidated than surficial sediments and therefore more resistant to erosion. However, spatially, the cores showed a high degree of variability with no apparent correlation with location within the LPR, organic carbon content, sand content, or bulk density; even duplicate cores taken at the same location showed a high degree of variability. Given this unexplained variability,

and the lack of any objective criteria to map this variability in erosion properties over the entire LPR domain, the erosion properties measured in the individual Sedflume cores were averaged to develop a single set of parameters for use in the LPR/NB model. Table 4 shows the erosion properties of the average core developed from the Sedflume data. These properties were assigned to the predominantly cohesive parts of the model domain: NB, the lower 8 miles of the LPR, and areas outside the former navigation channel above RM 8 in the LPR. Erosion properties for the predominantly non-cohesive parts of the domain (i.e., the areas within the navigation channel above RM 8, and all the areas above RM 13) were based on the values published in Roberts et al. (1998), which relates erosion properties to median diameter (D50) of the sediments.

Table 4. Erosion Properties for Parent Layers Derived from Sedflume data and Calibration

Depth Interval (cm)	A (cm/s)	N	τ_{Cr} (Pa)	
			Average of Data	6X, Calibrated
0 - 2.5	134×10^{-4}	2.14	0.1	0.61
2.5 – 5	62×10^{-4}	2.54	0.2	1.18
5 – 10	24×10^{-4}	2.71	0.31	1.85
10 – 15	24×10^{-4}	2.93	0.34	2.04
15 – 20	7.9×10^{-4}	3.25	0.53	3.17
20 – 25	4.4×10^{-4}	3.48	0.65	3.93
25 – 30	3.4×10^{-4}	3.39	0.69	4.17
>30	5.5×10^{-4}	2.79	0.54	3.25

Initial model runs using of the average core properties derived from the Sedflume data showed erosion on the order of 15-20 cm within the former navigation channel in much of the lower miles of the LPR even under normal tidal and below-average discharge conditions. This was an unexpected result since the erosion properties used to define the consolidated strata underlying the fluff layer were expected to result in a relatively stable bed under normal tidal and below-average discharge conditions. Furthermore, extending the initial application to the 16,000 cfs event on March 16, 2010 following an appropriate spin-up simulation resulted in significant over-prediction compared to the measured suspended solids data. Taken together, these results suggested an inconsistency between the shear stresses imposed by the model and the defined erosion properties of the parent layers, resulting in over-prediction of erosion under low as well as high-flow conditions. This result may likely be a consequence of under-estimating the critical shear stress for erosion. As shown in Figure 11, the critical shear stress computed using the approach

mentioned previously tends to under-estimate the empirical critical shear stress (the critical shear stress is bounded by the highest shear stress with no observed erosion and the lowest shear stress with some observed erosion) in each of the shear stress sequences run for the Sedflume cores. Therefore the critical shear stress of the parent layers was used as a calibration parameter and increased primarily to adjust the response of the model to the 16,000 cfs event of March 16, 2010. In particular, the shear stress profile of the average core calculated from the Sedflume cores was uniformly increased by a factor of 6; the resulting shear stress profile is also presented in Table 4. This approach to calibration and parameterization was chosen because it is consistent with the empirical critical shear stress data from the Sedflume tests and the resulting description of bed properties yields a state of quasi-equilibrium when combined with the model-predicted shear stresses under normal tidal and discharge conditions. A similar empirical approach for deriving the critical shear stress for erosion was also used in the Housatonic River ST model (Weston 2004).

Deposited Layers

The deposited layers refer to sediment layers developed by deposition during the course of the model simulation. At model initialization, only the parent layers and a fluff layer are defined. Following initialization, as the simulation progresses, any deposited sediments are tracked in a separate stack referred to as the deposited layers. This is purely a computational heuristic to allow newly deposited sediments to be tracked separately from the parent layer sediments, which are more consolidated than the freshly deposited sediments. The deposited sediment layers are subject to consolidation during the course of the simulation. The consolidation model follows Sanford (2008) and has been parameterized such that upon complete consolidation, the deposited layers reproduce the profile of erosion properties developed and calibrated for the parent layers (described in the preceding section). The consolidation rate associated with the transition from the freshly deposited, unconsolidated state to the completely consolidated state is based on the consolidation experiments performed using LPR sediments (SEI 2008).

3.2.5 Settling Velocity

The settling velocities associated with the individual sediment classes within the ECOM-SEDZLJS model are treated separately based on particle size. For the non-cohesive classes (diameter >63um), settling velocity is calculated by the model as a function of the particle diameter using the formulations in Cheng (1997). However, for the cohesive classes, given the influence of processes such as flocculation that are not included in the model, the settling velocity has to be specified as a site-specific input. The settling velocity of the clays and silts in the model were defined based on the analysis of data on the vertical distribution of suspended sediments and flow velocities from Sommerfield and Chant's (2010) data collection effort, and from the Fall 2009 PWCM program.

Ignoring effects on vertical mixing by vertical salinity gradients, and assuming small longitudinal gradients in flow and sediment concentrations, the vertical suspended

sediment profile is expected to follow the logarithmic Rouse distribution (Van Rijn, 1984). The bulk settling velocity estimates of the total suspended sediments were therefore derived from the parameters of the fit of the data to this vertical distribution. By computing the bulk settling velocity in a similar manner based on each vertical profile, the mean and median statistics were obtained over the entire time-series covered by each dataset. Figure 12 shows probability distributions of the calculated settling velocities at each of the mooring locations from the 2009 Fall PWCM program and the Sommerfield and Chant (2010) location at RM 1.4 in the LPR. The majority of the calculated settling velocities are in the 1-5 mm/s range, with medians computed at different stations along the river ranging from about 1.05 mm/s at RM 13.5 to about 2.6 mm/s closer to the mouth of the river; the down-estuary increase is attributed to tidal asymmetry, vertical mixing and sediment flocculation.. These computed settling velocity estimates were also found comparable also to the estimates from the EDPS experiment lending further credence to this analysis.

This analysis is inclusive of all the suspended sediment types and size classes within the water column, whereas one expects the distribution of settling velocities to be directly correlated with grain size diameters. Therefore the results from this analysis were used merely as a general guideline during the model calibration process. Calibration yielded constant settling velocities of 0.05 mm/s and 0.5 mm/s respectively for the clay and silt classes used in the ST model.

3.3 ECOM-SEDZLJS Code Modifications

As mentioned previously, model setup and calibration was an iterative process that included a number of modifications to the ECOM-SEDZLJS code received from EPA. Although the model algorithm has changed somewhat from the version received from EPA, the erosion, deposition, and consolidation formulations that are at the heart of the ECOM-SEDZLJS framework have not changed. Rather, the code modifications for the most part are incremental in nature and represent an enhancement of the model capabilities to ensure the reproduction of the key sediment transport processes that have been identified in the LPR (see Section 2). The code modifications fall into two broad categories: (1) related to the schematization of the bed layering, and (2) related to the decoupling of the hydrodynamic and sediment transport models and the bathymetric feedback between the decoupled models.

3.3.1 Schematization of Bed Layering

The model application to long-term periods involving a range of discharge conditions initially focused on the erosion properties of the parent layers. As described previously, the critical shear stress of the parent layers was adjusted through a process of calibration resulting in a sediment bed that is relatively stable during low discharge and normal tidal conditions, and which results in a good comparison of predicted and measured suspended sediment concentrations during high-flow conditions. The calibrated erosion properties are such that erosion from the parent layers and from the consolidated deposited layers

occurs primarily during episodic storm events. As a consequence, during low to average discharge and normal tidal conditions, the model did not reproduce processes such as the tidal variability, tidal pumping, infilling, and the exchange with Newark Bay. Since sediment transport under such conditions in the LPR is dominated by the dynamics of the fluff layer, and since the entrainment rate analysis provides information to support the parameterization of the fluff layer, the bed discretization in ECOM-SEDZLJS was modified to include the fluff layer. Similar schematizations of the bed involving a more erodible fluff layer overlying a more consolidated layer have been applied at other sites as well (El Ganaoui et al. 2004; Van Kessel et al. 2007).

Figure 13 shows a schematic of the revised bed layering along with a conceptual description of the hydrodynamic conditions that can potentially scour through the various strata. The fluff layer is located underneath the active layer (which is the layer at the interface between the bed and the water column) and is subject to erosion and deposition through the active layer. Under erosional conditions (e.g., the flood tide), the fluff layer may disappear due to resuspension. During the following depositional condition (e.g., slack water), the depositing sediments first recreate the fluff layer. When the fluff layer exceeds its pre-determined maximum thickness, the excess sediment is transferred to the underlying layer. Given the order of magnitude difference in strength between the fluff layer and the underlying parent or deposited layer, in order to avoid a discontinuity in strength and also for a better model-data comparison especially during spring tides, a transitional layer (same thickness as fluff layer) with intermediate strength was also introduced into the bed structure. New depositional layers are created immediately underneath the transitional layer, and under depositional conditions, sediment is transferred from the fluff layer through the transitional layer to the new depositional layer underneath. The deposited layers are subject to consolidation as described previously. Under erosional conditions, the layer depletion proceeds in a logical manner with the fluff layer eroded first, followed by the transitional layer and subsequently by the deposited or parent layer, as the case may be.

Additional minor code modifications made during the course of the CPG ST model development are listed below:

- The active layer assumes erosion properties (critical shear stress and erosion rate) of the bed layer it is exchanging sediments with. This can be either the fluff or transitional layer, or a deposited or parent layer, depending on the preceding history of deposition/resuspension.
- The time-variable behavior of the active layer as cohesive or non-cohesive (with respect to erosion properties), was modified to include a criterion based on the cohesive content being <15%, in addition to the original criterion of D50 being >200 um for the layer to be treated as non-cohesive.
- The D50 used for the calculation of skin friction from the total bed shear stress is based on the grain size distribution of the surficial sediments at model initialization rather than the time-variable grain size distribution within the active

layer, to prevent high frequency oscillations in the active layer composition from yielding unrealistic effects.

- The formation of bed forms and its effect on reducing skin friction was restricted to the part of the model domain defined as predominantly non-cohesive at model initialization, i.e. areas within the navigation between RM 8 and 13, and all the model cells above RM 13.
- The settling velocity of the cohesive classes was modified as a constant input value rather the concentration-dependent formulation originally implemented in the model.

3.3.2 Hydrodynamic and Sediment Transport Decoupling and Bathymetric Feedback

The ECOM-SEDZLJS code and inputs received from Region 2 were set up to simulate both hydrodynamics and sediment transport simultaneously. However, the runtime associated with coupled hydrodynamic and sediment transport runs was prohibitively long, on the order of about 2½ days per year of simulation. In an effort to reduce the ST model runtimes, and especially with respect to the long-term (15 years) simulations necessary for calibrating the ST and contaminant models, the hydrodynamics and sediment transport simulations were decoupled. The hydrodynamic model is run independently of the ST model and its transport solution saved as a 15-minute average during the course of the simulation. The ST model subsequently reads the saved hydrodynamic output and is run independently, with three times larger time-steps than the hydrodynamic model simulations, resulting in average runtimes of about 16 hours per year of simulation. ECOM-SEDZLJS already included the capability to run decoupled hydrodynamics and sediment transport; during the course of the CPG's application to the LPR and NB, this feature was tested and debugged.

In the ECOM-SEDZLJS code and inputs received from EPA, the bathymetric change computed by the sediment transport model in response to erosion and deposition during a given year is incorporated into the simulation of the following year. This feedback was approximated in the CPG's decoupled hydrodynamic and sediment transport runs by means of a continuity correction similar to the implementation in the Delft morphological sediment transport model (Delft 2001). Since the hydrodynamic run is performed only once using a certain bathymetry, the bathymetric changes computed by the sediment transport model are used to modify the previously generated hydrodynamic solution by adjusting the water depth in a given cell in response to the changing bathymetry while preserving the discharge through that model cell. This results in a modification of the velocity and shear stresses in that cell in a manner similar to what would be achieved if the hydrodynamic model were to be rerun with the revised bathymetry. For instance, a model cell experiencing deposition during the course of the ST simulation would see its velocity and shear stress increase as the water depth gets shallower. This approximation is valid so long as bathymetric changes are small relative to the total water depth. For example, it will not be appropriate in cases such as a remedial alternative for the LPR that involves dredging of the navigation channel down to the federally mandated depth, a change that would involve roughly doubling the water depths in some areas. In such

cases, the hydrodynamic model would need to be rerun with the post-dredge bathymetry in order to drive the ST model. Comparison of an ST model run using this approximation to a fully coupled hydrodynamic and ST model with periodic bathymetric feedback showed a generally good comparison between the two approaches in terms of the bathymetric changes predicted in a long-term simulation. Minor differences between the two approaches were explainable and reasonable.

4.0 MODEL CALIBRATION AND PERFORMANCE

The calibration of the LPR and NB ST model is an ongoing task. Certain elements of the calibration such as model-data comparisons of suspended solids and fluxes within the LPR may be considered better resolved than others; for example, the year-to-year bathymetric changes can only partly be resolved by the model, as a significant portion of these bed level changes occur at sub-grid scale in the model.

The calibration will be revisited as additional investigations are performed and model refinements are made. For example, the model inputs for Newark Bay relied on the LPR data due to a lack of erosion rate data in Newark Bay, but this data gap will be filled by recent field programs. Another example is the effects of wind-generated wave shear stress and shipping activities in NB, which have yet to be reviewed and incorporated in the model. Furthermore, some of the parameter calibrations were established before the implementation of model features such as the continuity correction to establish a feedback between the bathymetric changes computed by the ST model and the hydrodynamics and which have had subtle impacts on model performance. Therefore, it is anticipated that the parameter calibrations and therefore the model results presented in this document may be further refined.

This section describes the model calibration process, the calibration parameters, calibration metrics, and the model-data comparisons.

4.1 Calibration Parameters

The model inputs adjusted as part of the calibration process include the critical shear stress of the parent layers (and by extension also the deposited layers), the settling velocities of the clay and silt classes, and the fluff layer erosion properties in Newark Bay. As mentioned previously, the critical shear stress defined for the parent layers was calibrated in order to achieve a favorable comparison between the model calculations of suspended sediment concentrations, and the measurements during the 16,000 cfs event on March 16, 2010. The settling velocity of the clays and fines was calibrated primarily to reproduce the vertical profile of suspended sediment concentrations measured during the 16,000 cfs event on March 16, 2010 as well as the Fall PWCM data. It should be noted that settling velocity analysis needs to be updated with the revised EPA estimates of suspended sediment concentrations and the shear stresses that are an input to the settling velocity analysis also need to be updated following the changes to the model formulations for skin friction (bed form and smooth turbulence corrections). Finally, the erosion properties of the fluff layer in NB were adjusted in order to match the net flux measured at RM 1.4 in the Fall 2009 PWCM program, and by Sommerfield and Chant (2010); this was primarily achieved by increasing the erodibility (enhancing the erosion rate as well as reducing the critical shear stress) of the fluff layer in NB. It is anticipated that the parameterization of the model within NB may change following the completion of the system understanding of NB, the ongoing Sedflume data collection program in NB,

and the detailed ST model application in NB. Adjusting the erodibility of the fluff layer in NB is a temporary measure to achieve the right exchange with the LPR until the aforementioned refinements can be incorporated.

4.2 Calibration Periods

The model performance has been assessed by comparing model calculations to the following datasets, while the model settings obtained during calibration remain unaltered:

- Fall 2009 PWCM – suspended solids concentrations and net fluxes
- 16,000 cfs event on March 16 2010 – suspended solids concentrations
- Spring 2010 PWCM – suspended solids concentrations[3]
- Bathymetric changes over the periods covering the 2007-2008, 2008-2010, and 2010-2011 multi-beam surveys

Taken together, these model-data comparisons allow the assessment of model performance over a range of discharge conditions from low-flow conditions of ~100 cfs to the 16,000 cfs event on March 16 2010 (a 25 year event; MPI 2007b). Further, the comparison of predicted and measured bathymetric changes between the 2010 and 2011 multi-beam surveys also allows for an assessment of model performance during a period including an extreme event (Hurricane Irene), when discharge at Dundee Dam peaked at 24,000 cfs, approximately a 100-year event (MPI 2007b).

The results presented in this section are taken from a long-term simulation starting in October 1994 (Water Year 1995) and run through September 2011 (Water Year 2011). The hydrodynamic model was run using bathymetry developed by Region 2 to represent the 1995 time-horizon, with periodic updates to the bathymetry in NB and the Kills to incorporate the various maintenance and capital dredging projects in those areas during the simulation period. Bathymetric changes computed by the ST model were included by means of the continuity correction described previously, typically every 15 days during the simulation and more frequently during storm events.

4.3 Model-Data Comparisons

4.3.1 Suspended Solids Concentrations, Fall 2009 PWCM

Figure 14 through Figure 18 show model-data comparisons of salinity, depth-average, and surface and bottom suspended solids concentrations at RMs 1.4, 4.2, 6.7, 10.2, and 13.5 during the Fall 2009 PWCM period. In general, the model reproduces the major

[3] Pending review and finalization of the ABS-derived suspended solids data for the Spring 2010 PWCM survey, the Spring 2010 PWCM data presented in this document are restricted to the suspended sediment concentration estimates from the measurements of optical backscatter (OBS). Since only surface and bottom OBS measurements were made, suspended sediment fluxes cannot be estimated. Therefore, the model-data comparisons are restricted to suspended sediment concentrations.

features noted in the data: intra- and inter-tidal (spring-neap) variability in suspended sediment concentrations as well as the presence of an ETM associated with the salt front. Although most model calculated suspended sediment concentrations are within a factor of two of the measured values, certain consistent patterns are apparent in the model-data comparisons. At all locations that are predominantly within the salt-wedge during the course of the deployment (RMs 1.4, 4.2, and 6.7), the model predictions are either comparable or somewhat lower than the depth-average suspended sediment concentrations during the neap tides (around Oct. 28, Nov. 13, and Nov. 25); salinity calculations from the hydrodynamic model during the same periods also tend to show a bias towards under-prediction suggesting that the bias in the ST model calculations may be due to a bias in the hydrodynamic model. In contrast, during spring-tides (around Oct. 18, Nov. 5, Nov. 18, and Dec. 4), the model generally tends to over-predict the depth-average suspended sediment concentrations during the flood tide and therefore the intra-tidal variability at RM 1.4. However, at RM 4.2, during the spring tide on Oct 18 when the ETM is located upstream, the model generally tends to under-predict, whereas it is more comparable to the data during the spring tides on Nov. 5, Nov. 18, and Dec. 4 when the ETM is in the vicinity of this location. At RM 6.7, during all four spring tides listed above, the ETM is in the vicinity of this location and the model generally tends to over-predict the depth-average suspended sediment concentrations. At RM 10.2, before the spring tide around Oct. 18, the model agrees well with the measured suspended sediment concentrations; however, during the following spring tide the model tends to over-predict the suspended sediment concentrations. During the remainder of the deployment at RM 10.2 the model and data agree well, although the model does not show as much intra-tidal variability as noted in the data. . Model predicted concentrations at RM 13.5 are generally biased high compared to the data. This may be an artifact of the boundary condition imposed at Dundee Dam. The current model setup involves the use of a rating curve to define the solids concentration associated with the Dundee Dam discharge. Since the PWCM deployments also included a mooring at Dundee Dam, an alternative that could help improve model-data comparisons, especially at RM 13.5, would be to use the measured Dundee Dam concentrations to define the inflowing solids concentrations.

There may be a number of reasons for the discrepancies noted between the model and data including, (1) assumptions regarding the grain size distribution of the water column boundary condition at Dundee Dam and the other freshwater boundaries, (2) calibration of the exchange between the LPR and NB which was established before the inclusion of the bathymetric feedback between the hydrodynamic and ST models via continuity correction, (3) bias and artifacts associated with the hydrodynamic model, (4) artifacts associated with the ABS data and ABS derived suspended solids concentrations received from EPA in 2010 (revised values received from EPA are currently under review, and may change the conclusions regarding the model-data comparisons.) These discrepancies and potential factors noted above will continue to be investigated in order to refine the ST model performance.

4.3.2 Suspended Solids Concentrations, High Flow Conditions

Figure 19 shows model-data comparisons of suspended solids for the three longitudinal transects in the LPR and NB measured by Dr. Bob Chant, and for the water sample data collected by the CPG during the 16,000 cfs event on March 16, 2010. This was a 25-year event (MPI 2007b) and represents the model calibration under high-flow conditions. The data collected by Dr. Bob Chant includes vertical profiles of suspended solids concentrations at several locations along the thalweg in the LPR and within the navigation channel in NB whereas the data collected by the CPG represents samples from the surface of the water column.

Although biased towards over-prediction, most calculated values are within a factor of two of the measured values, especially for transects 1 and 3. In addition to over-predicting erosion, the model results may also be biased high because of assumptions regarding the composition of the solids loading from Dundee Dam. The current setup assumes that all of the cohesive solids loads from Dundee Dam are clays, which have relatively low settling velocities. While this assumption may be reasonable for below-average flow conditions, during high-flow conditions it may not be an accurate assumption. During high-flow events, the particle sizes in suspension as well as their settling velocities would be expected to be higher than during below-average flow conditions. The sensitivity of the model results to the assumptions regarding composition of the Dundee Dam solids loading was explored by performing a sensitivity run with the cohesive solids loading at Dundee Dam assigned to the silt class. The resulting model predictions are more comparable to the data, especially at measured values <~100 mg/L which are predominantly from locations in Newark Bay and/or near the surface of the water column. Similar to the distribution of the cohesive loadings into the clay and silt classes, the distribution between cohesive and non-cohesive loadings from Dundee Dam and the other freshwater tributaries can also influence the model-data comparisons. Therefore, the grain size distribution associated with the freshwater boundaries will be a continuing area of focus, with a potential refinement possible using proposed measurements of the water column grain size distribution at several discharge conditions.

4.3.3 Suspended Solids Concentrations, Spring 2010 PWCM

Figure 20 through Figure 24 show model-data comparisons of salinity, depth-average, and surface and bottom suspended solids concentrations at RMs 1.4, 4.2, 6.7, 10.2, and 13.5 during the Spring 2010 PWCM period. The estimates of surface and bottom suspended sediment concentrations are based on measurements from the OBS sensor which represents a point measurement 3 feet above the bed and 3 feet below the surface respectively. In contrast, the model calculation represents an average over a sigma-level within the water column, a depth interval of 1-2 feet resulting in a mismatch between the model and data. The OBS sensors were subject to some fouling – the gaps in the data record indicate periods when the data were considered to be affected by sensor fouling. Nonetheless, the OBS data are used for a general comparison of the trends and comparison between model and data.

Model-data comparisons are quite favorable at RM 13.5 over the entire deployment. However, over-prediction of erosion between RMs 13.5 and 6.7 during the 10,000 cfs event in late March/early April causes a discrepancy between model and data that is also reflected at RM 4.2; the over-prediction is currently under investigation. Following the high-flow period at the beginning of the deployment, model calculations are generally comparable to measured values. It is anticipated that the ABS-estimates of suspended solids will help to better resolve these discrepancies, define the solids profile within the water column, as well as avoid some of the limitations of the OBS measurements such as a bias associated with the particle size of the sediments in suspension. The model performance during the Spring PWCM period will be evaluated in greater detail once the ABS-derived suspended solids estimates are finalized.

4.3.4 Net Suspended Solids Fluxes, Fall 2009 PWCM

Figure 25 through Figure 29 show model-data comparisons of the direction and magnitude of the net solids flux as a function of discharge for the Fall 2009 PWCM period. The model calculated flux at each mooring location has been normalized to the cell width for an equivalent comparison to the PWCM data. These comparisons show that, in general, the model successfully captures the process of tidal pumping within the LPR as well as the exchange between the LPR and NB. Although the exchange between the LPR and NB as characterized at RM 1.4 is more variable in the model than the data, the general trend is comparable. With the exception of RM 6.7, the direction and magnitude of the fluxes and its dependency with discharge at all the other locations compare quite well with the data. At RM 6.7, the magnitude of the fluxes during periods when the net flux is directed down-estuary is under-represented in the model. These discrepancies appear to be associated with the discharge events starting in early December 2009. Similar comparisons are yet to be performed for the Spring 2010 PWCM periods pending review of the ABS-estimates of suspended solids developed by EPA.

4.3.5 Bathymetric Changes

Figure 30 through Figure 32 show the bathymetric change measured in the 2007-2008, 2008-2010, and 2010-2011 multi-beam surveys (left panels), and model calculations during the corresponding periods within the lower miles of the LPR. The bathymetric difference data were averaged over the model cells, and only cells with at least 50% areal coverage in the bathymetry are presented. These bathymetric comparisons span low-flow years (2007-2008), and high flow years (2008-2010, and 2010-2011) showing distinct spatial patterns of erosion and deposition. A separate analysis of the year-to-year bathymetric change observed in these multi-beam surveys has shown the presence of several areas that behave in a cyclical manner, with erosion during high-flow periods and infill during low-flow periods. These areas are typically in the vicinity of bridge abutments or features such as river bends. However, the spatial scale of these features is too small to be resolved by the hydrodynamic and ST model grid. Therefore, in the

comparisons of model and data, the model is expected to under-represent these erosional features and therefore also the associated depositional features. Pending the outcome of an ongoing effort to identify the contribution to erosion and deposition from these cyclical areas, the model-data comparisons of bathymetric change are mainly intended for a high-level comparison of the spatial patterns of erosion and deposition.

During low-flow conditions (2007-2008; Figure 30), above RM 2, model and data are in general agreement with small areas of accumulation around RM 7.5, RM 6, and RM 4.5 and relatively low accumulation everywhere else. Below RM 2, the data show several areas of erosion whereas the model is generally depositional. Examination of the shear stress maps generated from the high resolution hydrodynamic model suggests that this erosion may be for reasons other than normal tidal hydrodynamics. In particular, the effect of ongoing shipping activities within the LPR (and NB) on shear stresses and resuspension patterns may be influencing the comparison, and will be investigated in future analyses. Model-data comparisons during the high-flow years (2008-2010 which included the 16,000 cfs event in March 2010, and 2010-2011 which included Hurricane Irene) are more favorable. During 2008-2010 (Figure 31), both model and data show limited areas of erosion above RM 2, and depositional areas in the stretch below RM 2. Given the higher discharge during Hurricane Irene, data show erosion down to RM 1.4 whereas the model shows erosion extending about 0.5 mile further down-estuary, with accumulation below RM 0.9 in both model and data (Figure 32). These spatial patterns of erosion and deposition suggest a broad agreement between the measured bathymetric changes and calculated values, with isolated aspects such as the erosion during 2007-2008 below RM 2 subject to further analysis and refinement in the model.

4.4 Model Validation: Simulation of Historical Infilling

In addition to the model-data comparisons during the periods covering the PWCM program and the recent multi-beam bathymetries, the model was applied for a qualitative test of its ability to represent the historic infilling of the LPR following the last major dredge event in 1949. Another reason for the relevance of this test is that one of the remedial alternatives under consideration involves the dredging of the lower 2 miles of the LPR to the federally mandated channel depth. Given the historical infilling of the LPR since the last major dredging event, a similar infilling response can be expected following another dredging event in the future.

Given the computational burden associated with this particular simulation, it was only run for 16 years, using boundary conditions identical to that used for the long-term calibration run (from Water Year 1995 through Water Year 2010) described in the preceding section. The distribution of discharge during this 16-year period is comparable to the long-term record at Little Falls suggesting its suitability for long-term model applications beyond the window of short-term model-data comparisons. The hydrodynamic and ST models were run decoupled, with periodic bathymetric feedback based on erosion and deposition calculated by the ST model explicitly (rather than by means of the continuity correction) incorporated into the hydrodynamic model

simulations of subsequent years. This bathymetric feedback occurred typically every 15 days during the simulation, and more frequently during storm events. The ST model parameterization was based on the calibration described in the preceding section.

The model bathymetry used for this simulation is an approximation of the conditions in the LPR, NB, and the Kills around the time of the last major dredge event in 1949 within the LPR. Bathymetry within the LPR was set to the federally mandated navigation channel depths (RM 0-2.6: 30 ft., RM 2.6-4: 20 ft., RM 4-7.8: 16 ft., RM 7.8-Dundee Dam: 10 ft.; depths relative to MLW). Within NB and the Kills, the bathymetry was approximated based on maps showing the historical evolution of Newark Bay (USACE 2006). Major features represented accordingly are a 30 ft. (relative to MLW) channel in the Kills leading to Port Newark and the LPR, and the absence of the Port Elizabeth, Port Elizabeth pier head, and Port Elizabeth channels; the bathymetry in these areas was set at 5 ft. (relative to MLW).

The results from this simulation and its comparison to the measured infill are shown in Figure 33. Between RM 2.5 and 6.8, the measured historical infill is calculated by comparing the 1949 and 2010 bathymetries, and below RM 1.4 it is calculated by comparing the 1983 post-dredge bathymetry to the 2010 bathymetry. The bathymetric change for both model and data panels are presented as an annualized sedimentation rate. Both data and model show much higher infill rates near the mouth of the LPR than at locations further up-estuary. Above RM 2.5, both the model and data show relatively high infill rates along the southern edge of the navigation channel between RM 2.5 and 3.2, and in the inner bend at RM 4, and towards the shoal at RM 4.2. Similarly, both the model and data show lack of infill in the bend at RM 4.7, and in the vicinity of the Bridge St, Clay St, and I280 bridges (RM 5.5-6.5). Notable locations with a discrepancy between model and data include the vicinity of RM 5, RM 7, and the inner bend at RM 3.5.

An exact match is not to be expected between the model and the data for several reasons, including: (1) the system never had a bathymetry as exactly simulated with the complete mandated navigation channel all dredged at the same time, (2) differences between the actual hydrograph during the years spanning the data and the hydrograph used in the model, lack of information on the historical solids loadings, and (3) differences in sedimentation rate over time (sedimentation rates would be expected to be highest during the period immediately following dredging and decrease subsequently). Rather, this comparison is mainly for a qualitative assessment of the predicted patterns of infilling, and for a high-level assessment of whether the model as formulated and parameterized is capable of reproducing the infill expected following a dredging event. Looking ahead, a similar evaluation can be made with regard to the model's ability to calculate the infill within the navigation channel in Newark Bay and its removal through maintenance dredging, a quantity that can potentially be used as a calibration metric for the model in Newark Bay during future refinements. Nonetheless, in general, the present version of the model favorably reproduces the infill process that has been historically observed within the LPR.

5.0 SUMMARY AND NEXT STEPS

The model performance presented in this document suggests a broad agreement between the model and data within the LPR. The model performance has been compared to a number of datasets and metrics such as the suspended sediment concentrations, water column sediment fluxes, and the short-term and long-term bathymetric changes. Model-data comparisons have also been performed over a range of flow conditions ranging from low-flow to extreme event conditions (Hurricane Irene, a 100-year event). In general, the model reproduces the major processes identified in the data such as the intra- and inter-tidal variability, tidal pumping, exchange with Newark Bay, scour associated with episodic storm events, and infilling. Nonetheless, as described below, several tasks are ongoing or planned in order to advance and refine the ST model calibration and performance within the LPR as well as in NB.

One ongoing task is the review of the revised ABS-estimates of suspended sediment concentrations from the Fall 2009 and Spring 2010 PWCM surveys. The main issue is with respect to the use of separate regressions of ABS and suspended solids concentrations during high and low-flow periods. As a result, the time-series of ABS-estimated suspended solids concentrations show abrupt discontinuities during the transition from high-flow to normal/low-flow periods during the Spring 2010 PWCM deployment. Ongoing efforts in this regard relate to the development of alternative ABS and suspended solids relationships that do not produce discontinuities in the time-series of ABS-estimated suspended solids concentrations. Although the model parameterization could potentially change slightly as a result of the changes to the PWCM data and consequently the various data analyses that rely on the PWCM data, the model framework, in particular the model's schematization of the bed structure, and the sediment transport processes to be simulated by the model are not anticipated to change significantly. In addition to the PWCM data, additional model-data comparisons using the data collected by Sommerfield and Chant (2010) at RM 1.4, data collected by Rutgers University at RM 4.2, and data collected by Tierra Solutions in summer 2009 will be performed.

Another ongoing task is the further analysis of the year-to-year bathymetric change using the multi-beam bathymetry data. As previously noted, these data suggest the presence of several sub-grid scale features, typically in the vicinity of bridge abutments or features such as river bends, that behave in a cyclical manner, with erosion during high-flow periods and infill during low-flow periods. Since the ST model cannot reproduce these sub-grid features without major changes to model resolution and structure, efforts to identify the contribution to erosion and deposition from these cyclical areas are currently underway. It is anticipated that insights regarding these sub-grid features can subsequently be incorporated in the assessment of model performance and comparison to the bathymetric survey data.

The grain size distribution associated with the inflowing solids at Dundee Dam and the other freshwater tributaries as well as the open boundaries at the Kills is not well characterized and represents a data gap for both system understanding as well as model development. Ongoing efforts in this regard relate to measuring the grain size distribution in the water samples collected as part of the Chemical Water Column Monitoring program which involved several events ranging from ~300 cfs to ~2,500 cfs at Dundee Dam. It is anticipated that the data thus obtained will provide information to refine the grain size distribution associated with the inflowing boundary solids in the model, thus addressing one of the current sources of uncertainty in the model calibration and performance.

The remaining major area of focus in the development of the LPR and NB ST model pertains to the development of system understanding of sediment transport in Newark Bay, and the development and calibration of the model to Newark Bay. It is also anticipated that the availability of additional Sedflume data in Newark Bay (SEI and LBG 2012) will contribute to the refinement of the model. Following the review and inclusion, as necessary, of secondary processes such as wind-waves and shipping activities on shear stresses and sediment resuspension in Newark Bay, it is anticipated that the exchange between the LPR and NB will be better resolved than the current approximation which relied on calibrating the erodibility of the fluff layer in NB to the measured suspended sediment fluxes at RM 1.4 in the LPR.

Finally, the contaminant fate and transport model of the LPR and NB is still under development. As with the development of similar models at other contaminated sediment sites, it is possible that the ongoing development of the contaminant fate and transport model may necessitate further refinement of the ST model.

6.0 REFERENCES

AECOM 2010. Low Resolution Coring Characterization Summary. Lower Passaic River Study Area RI/FS

Borrowman, T.D., E.R. Smith, J.Z. Gailani, and L. Caviness, 2006. Erodibility Study of Passaic River Sediments Using USACE Sedflume. ERDC, US Army Corps of Engineers

Chant, R.J., D. Fugate, and E. Garvey, 2011. The Shaping of an Estuarine Superfund Site: Roles of Evolving Dynamics and Geomorphology. Estuaries and Coasts, 34 (1) pp 90-105

Cheng, N.S., 1997. Simplified Settling Velocity Formula for Sediment Particles, ASCE Journal of Hydraulic Engineering, 123, 149-152

CLH 1995. Work Plan, Vol. 1 of Passaic River Study Area Remedial Investigation Work Plans. Chemical Land Holdings (now Tierra Solutions, Inc.), Newark, NJ

Delft, 2001. Delft3D-MOR User Manual Ver. 3. Delft, The Netherlands

Dyer, K.R., 1997. Estuaries: A Physical Introduction, 2nd Edition, John Wiley & Sons

El Ganaoui, O., E. Schaaff, P. Boyer, M. Amielh, F. Anselmetc, and C. Grenz, 2004. The Deposition and Erosion of Cohesive Sediments Determined by a Multi-Class Model. Estuarine, Coastal and Shelf Science 60 pp. 457–475

HydroQual, 2006a. Final Modeling Work Plan. Lower Passaic River Restoration Project. Mahwah, NJ

HydroQual, 2006b. Final Modeling Work Plan Addendum. Newark Bay Study. Mahwah, NJ

HydroQual, 2008. Final Hydrodynamic Modeling Report. Lower Passaic River Restoration Project and Newark Bay Study. Mahwah, NJ

Jones, C. and W. Lick, 2001. SEDZLJ. A Sediment Transport Model. University of California, Santa Barbara, CA

Maa, J.P.Y., L. Sanford, J.P. Halka, 1998. Sediment Resuspension Characteristics in Baltimore Harbor, Maryland. Marine Geology 146 pp. 137-145

Malcolm Pirnie Inc (MPI), 2007a. Draft Environmental Dredging Pilot Study Report. Lower Passaic River Restoration Project and Newark Bay Study. White Plains, NY

Malcolm Pirnie Inc (MPI), 2007b. Draft Source Control Early Action Focused Feasibility Study. White Plains, NY

Mathew, R., D. Manian, R. Caizares, M. Greenblatt, K. Cadmus, J. Winterwerp, 2011. Sediment Transport Processes in the Lower Passaic River Study Area. 6th International Conference on Remediation of Contaminated Sediments, New Orleans, LA

Roberts, J., Jepsen, R., Gotthard, D. and Lick, W., 1998. Effects of particle size and bulk density on erosion of quartz particles. Journal of Hydraulic Engineering-ASCE, 124(12) pp. 1261-1267

Sanford, L.P., 2008. Modeling a dynamically varying mixed sediment bed with erosion, deposition, bioturbation, consolidation, and armoring. Computers & Geosciences 34 pp. 1263–1283

SEI. 2008. DRAFT: Sedflume Consolidation Analysis Passaic River, New Jersey. Prepared by Sea Engineering Inc. for Hydroqual, Inc. and U.S. Environmental Protection Agency. Santa Cruz, CA

SEI and LBG, 2012. Final Quality Assurance Project Plan for Sediment Erosion Rate Measurements in the Newark Bay Study Area. Santa Cruz, CA and Elmsford, NY

Sommerfield, C.K. and R.J. Chant, 2010. Mechanisms of Sediment Trapping and Accumulation in Newark Bay, New Jersey: An Engineered Estuarine Basin. Final Report to the Hudson River Foundation, University of Delaware, DE and Rutgers University, NJ

US Army Corps of Engineers (US ACoE), 2006. Geomorphological/Geophysical Characterization of The Nature and Dynamics of Sedimentation and Sediment Transport in Newark Bay focusing on the Effects related to Continued and Future Federal Navigation Channel Deepening and Maintenance. New York, NY

Van Kessel, T., H. Winterwerp, B. Van Prooijen, M. Van Ledden, and W Borst, 2007. Modeling the Seasonal Dynamics of SPM with a Simple Algorithm for the Buffering of Fines in a Sandy Seabed. INTERCOH, Brest, France

Van Rijn, LC, 1984. Sediment Transport, Part II: Suspended Load Transport. Journal of Hydraulic Engineering. 110 (11), pp. 1613-1641

Wang, Y.H. 2003. The Intertidal Erosion Rate of Cohesive Sediment: A Case Study from Long Island Sound. Estuaries, Coastal and Shelf Science 56 pp. 891-896

Weston Solutions Inc. 2004. Model Calibration: Modeling Study of PCB Contamination in the Housatonic River. Prepared for U.S. Army Corps of Engineers, and the US EPA

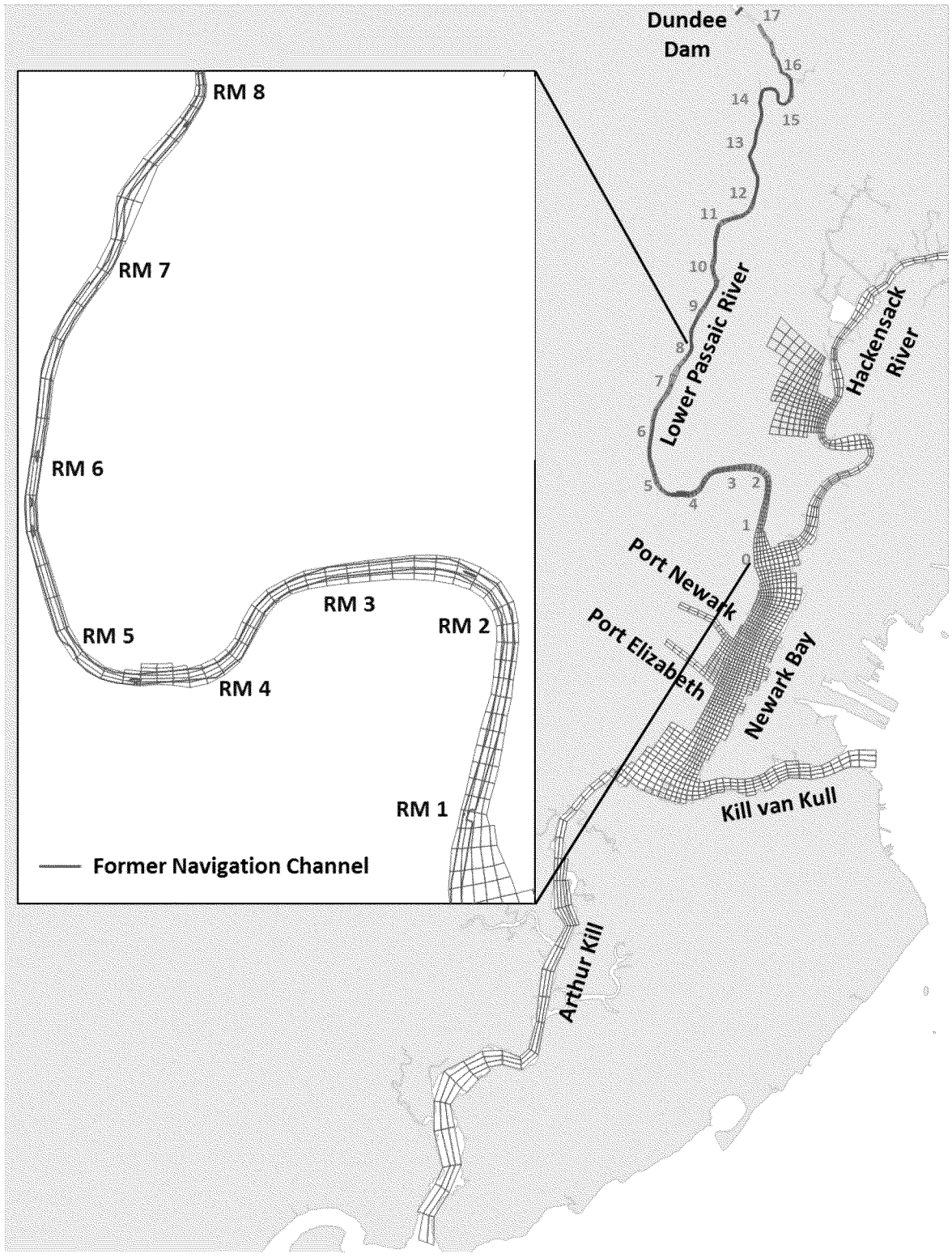

Figure 1. The Lower Passaic River and Newark Bay modeling domains, along with the computational grid for ECOM-SEDZLJS

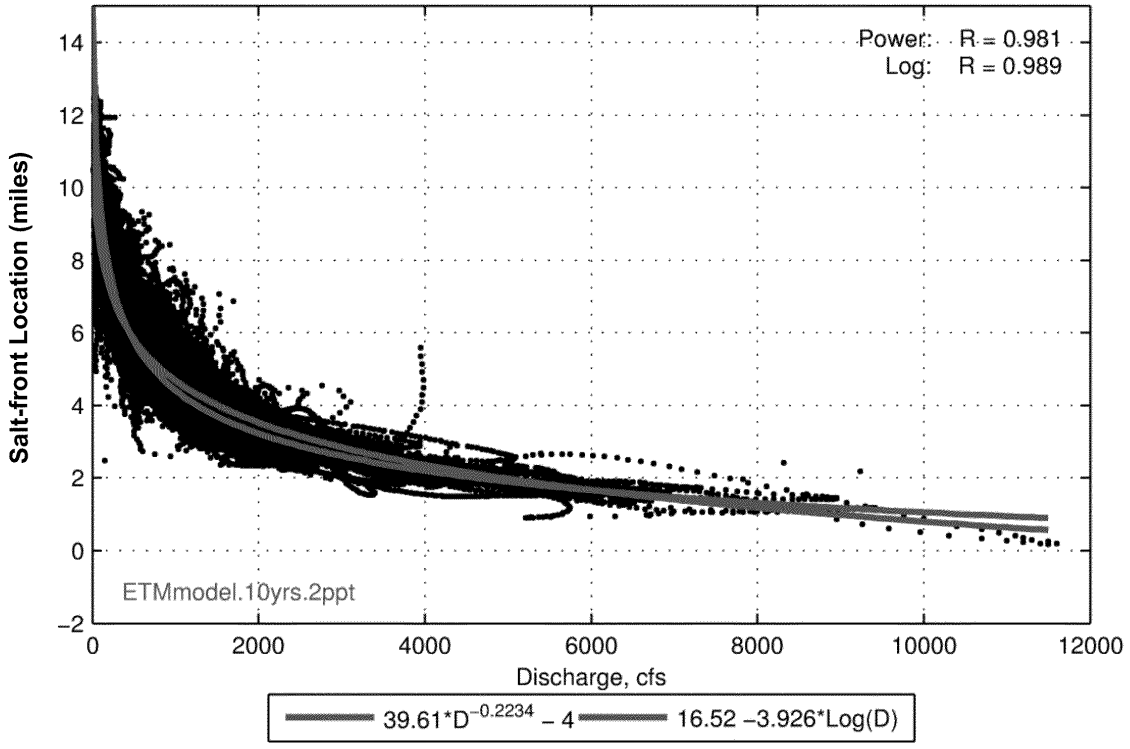

Figure 2. Salt front (defined as 2 ppt at the bottom of the water column) location as a function of discharge at Dundee Dam

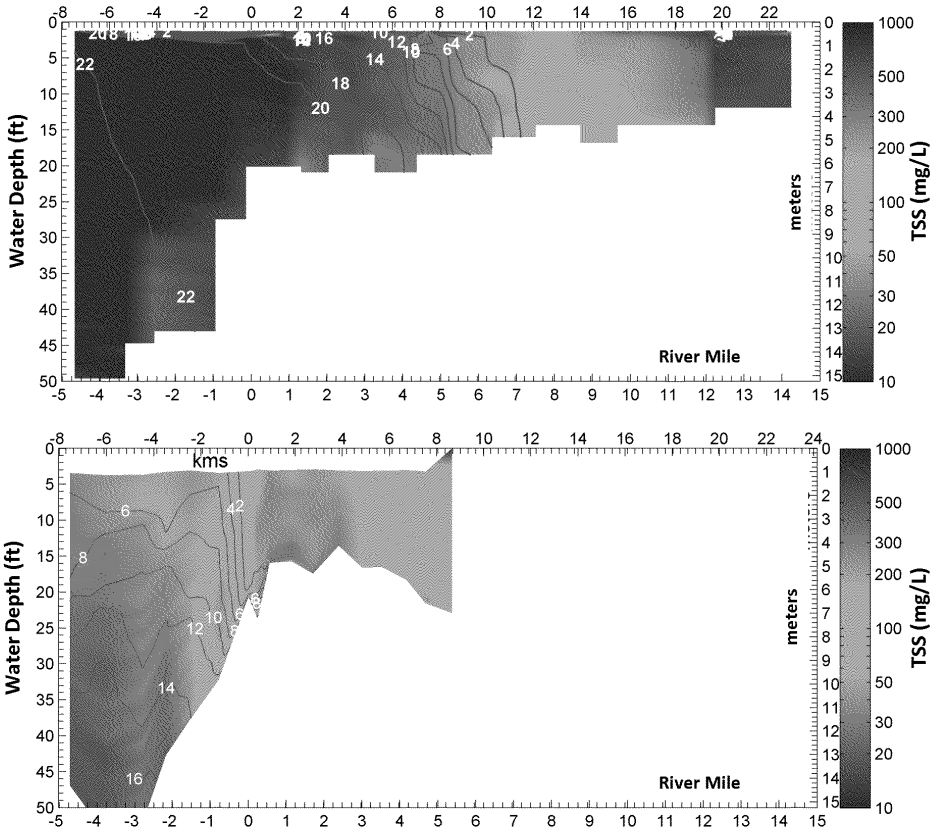

Figure 3. Longitudinal transects of salinity and suspended sediment concentration for a low-flow condition (250 cfs on June 23, 2005; upper panel) and for a high-flow condition (16,000 cfs on March 16, 2010; bottom panel)

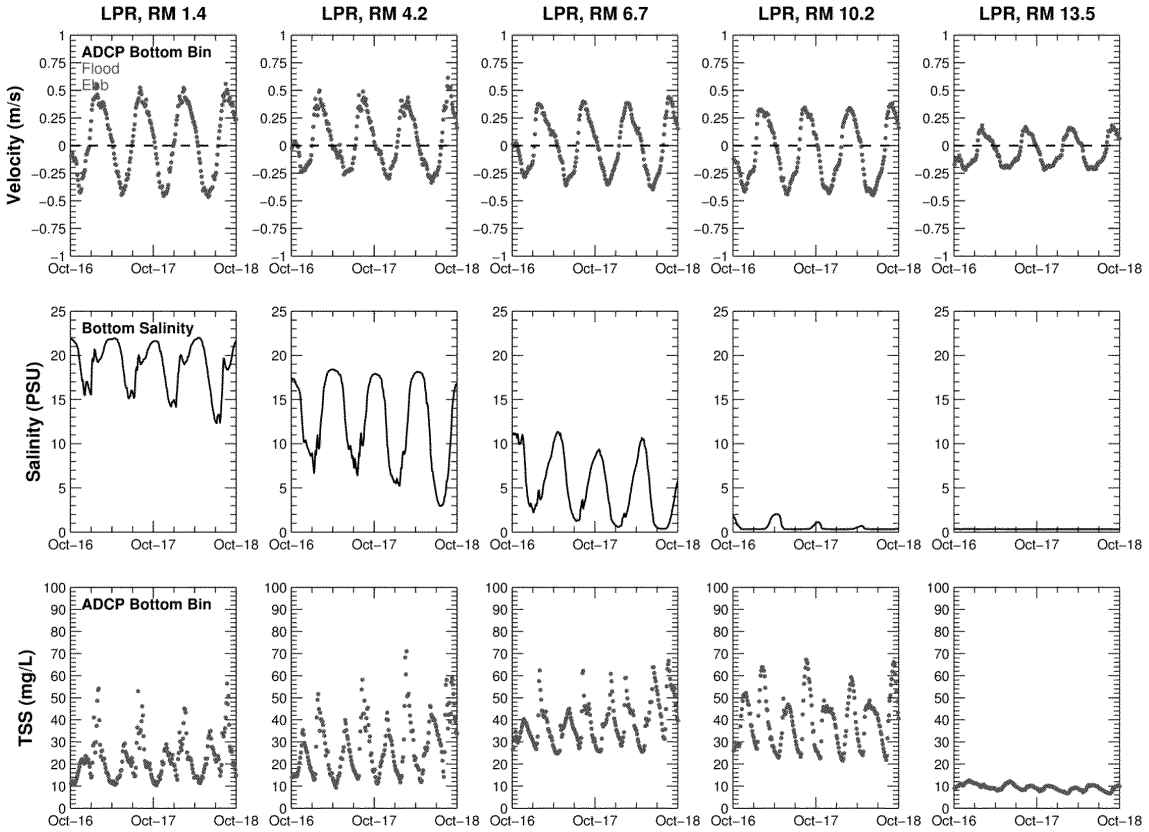

Figure 4. Near-bottom salinity, velocity, and suspended sediment concentration measured at RM 1.4, 4.2, 6.7, 10.2, and 13.5 during the Fall PWCM

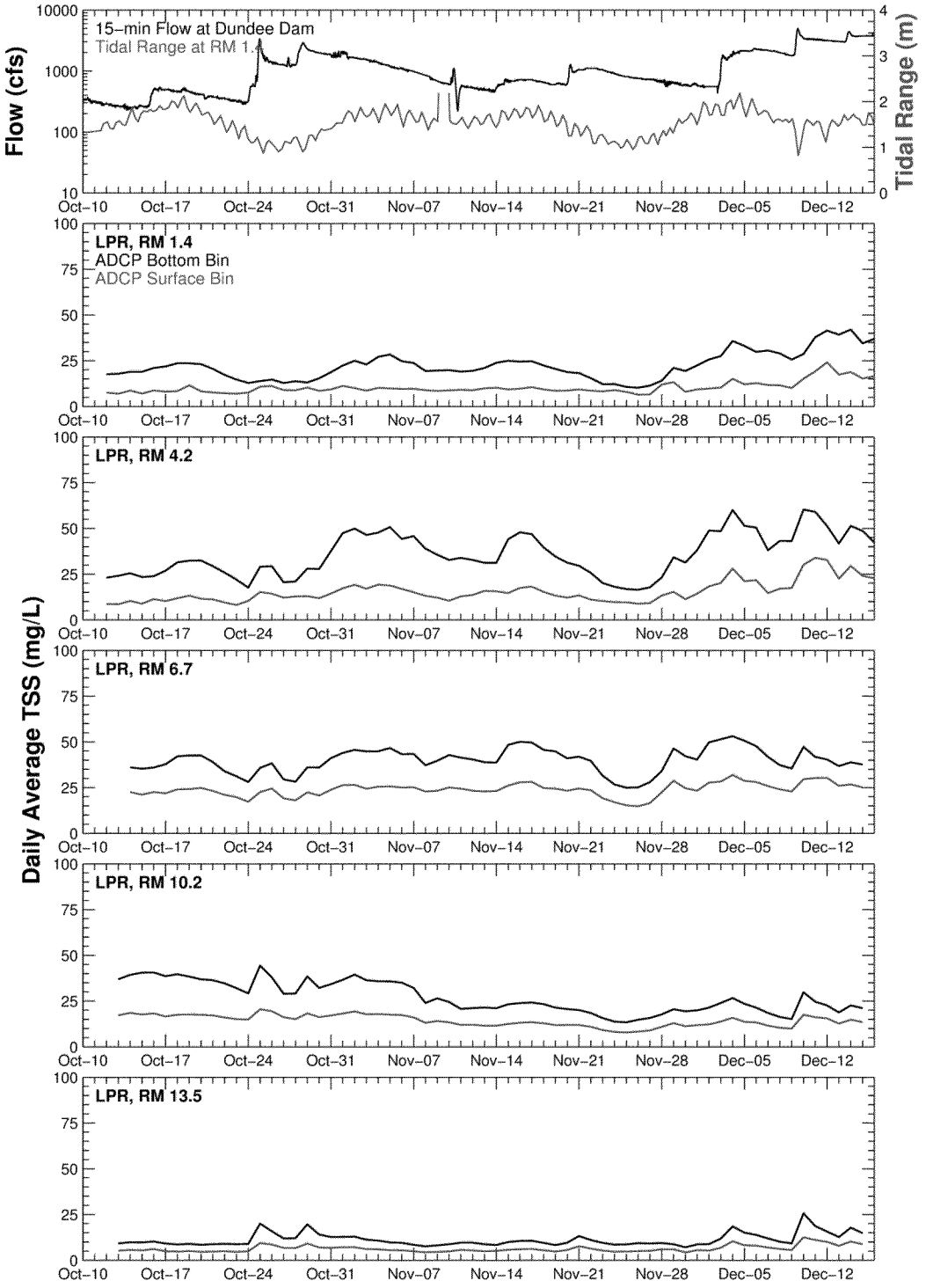

Figure 5. Inter-tidal variability in suspended sediment concentration, its relationship to the spring-neap cycle and discharge. From top to bottom, panels for RM 13.5, 10.2, 6.7, 4.2, and 1.4. Data from Fall 2009 PWCM

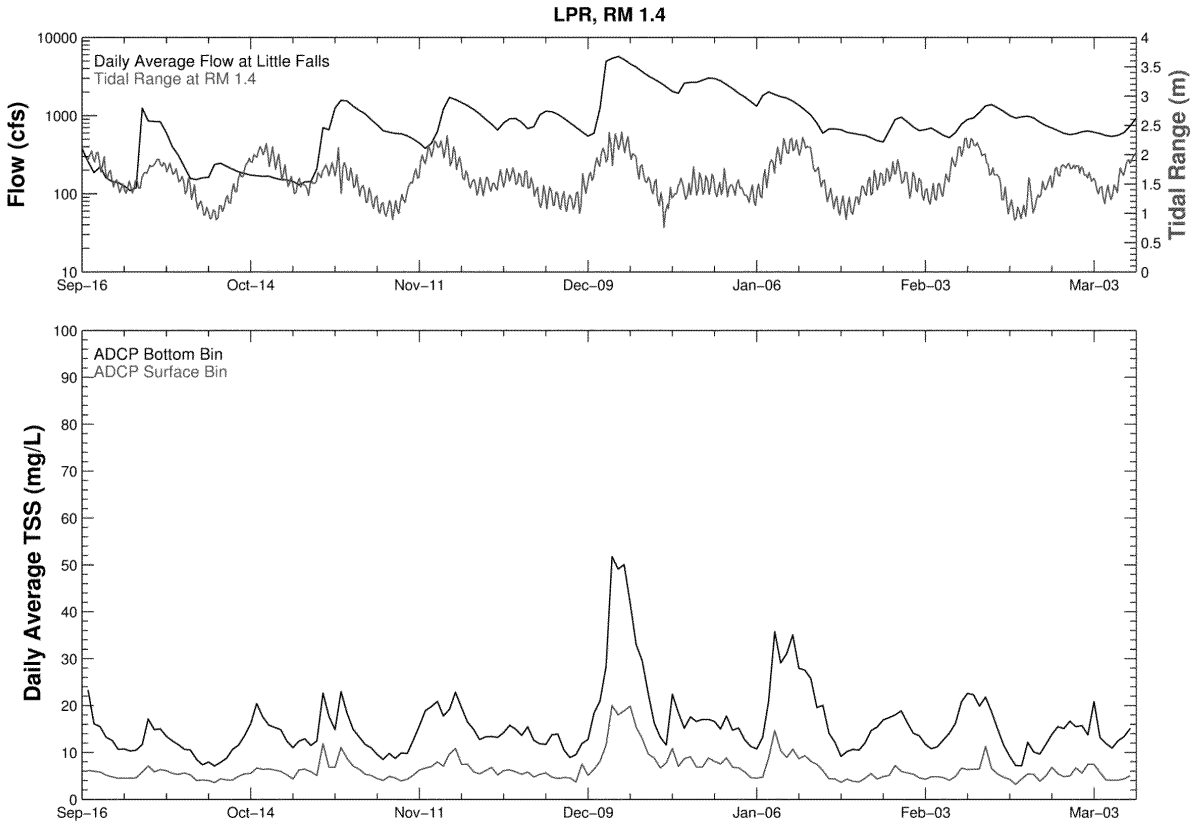

Figure 6. Inter-tidal variability in suspended sediment concentration, its relationship to the spring-neap cycle and discharge. Data from Sommerfield and Chant (2010)

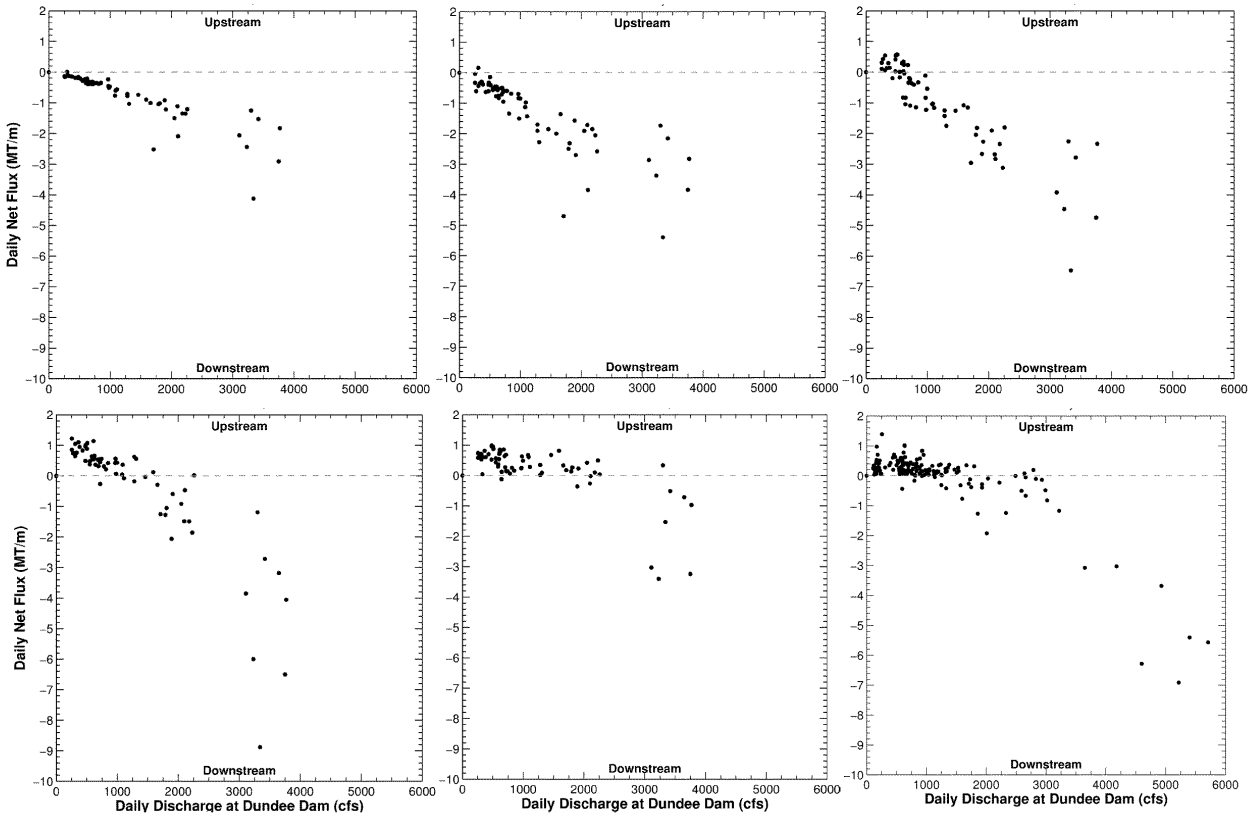

Figure 7. Net solids flux versus discharge. Upper panels from left to right - RM 13.5, 10.2, and 6.7 from Fall 2009 PWCM. Lower panels from left to right - RM 4.2 and 1.4 from Fall 2009 PWCM, and RM 1.4 from Sommerfield and Chant (2010)

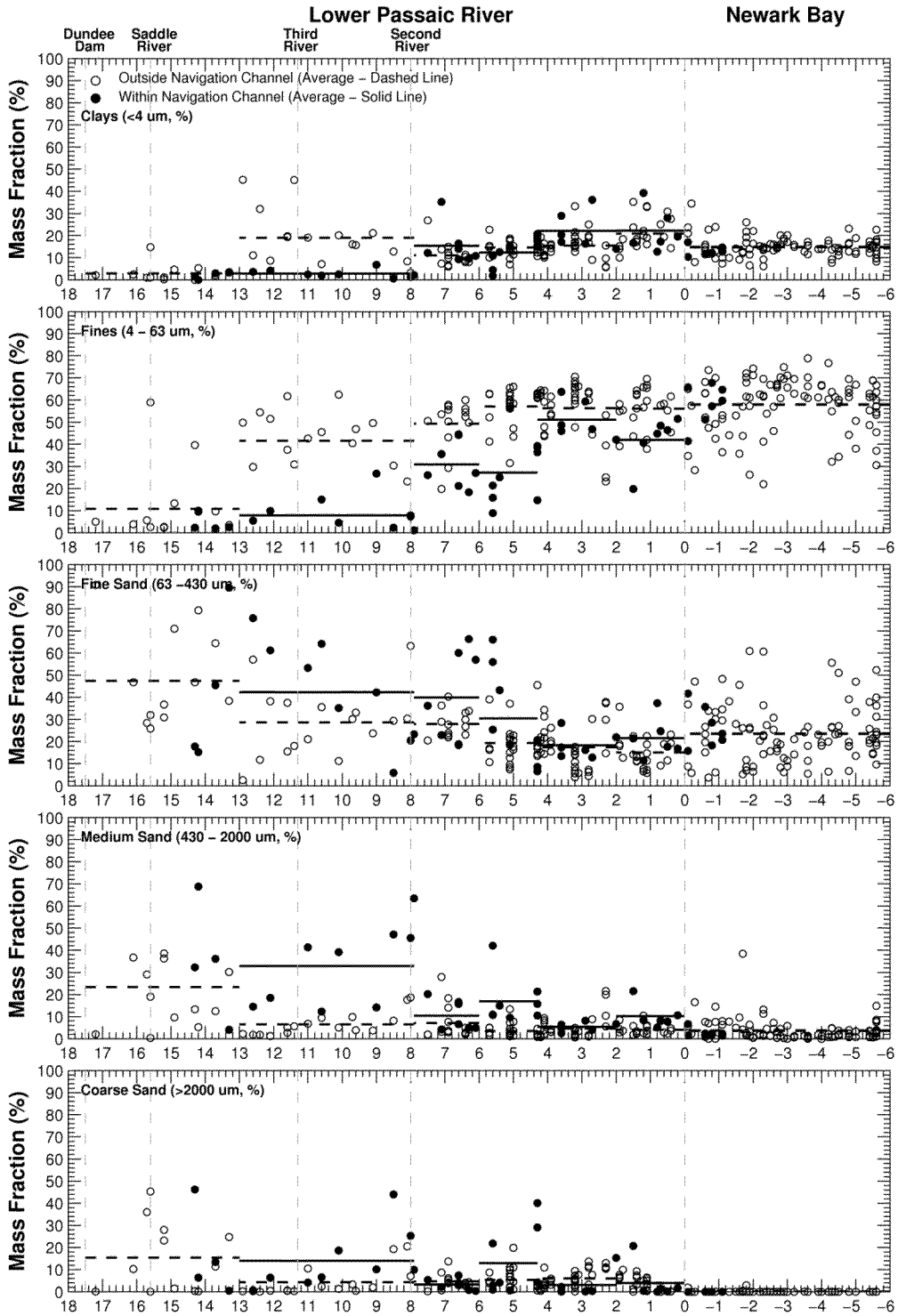

Figure 8. Longitudinal plot of grain size distribution data and model initial condition for surficial sediments (top 6" of bed)

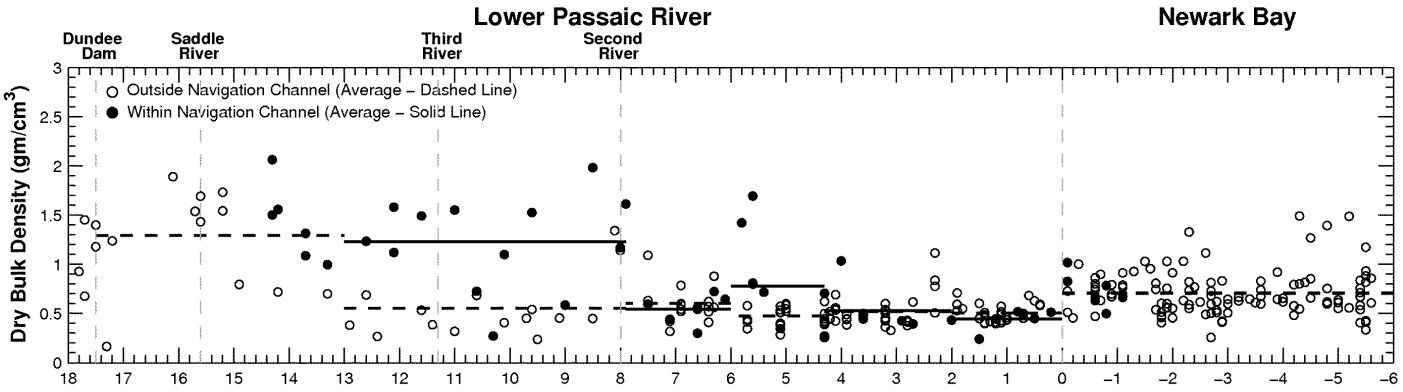

Figure 9. Longitudinal plot of dry density initial condition for surficial sediments (top 6" of bed)

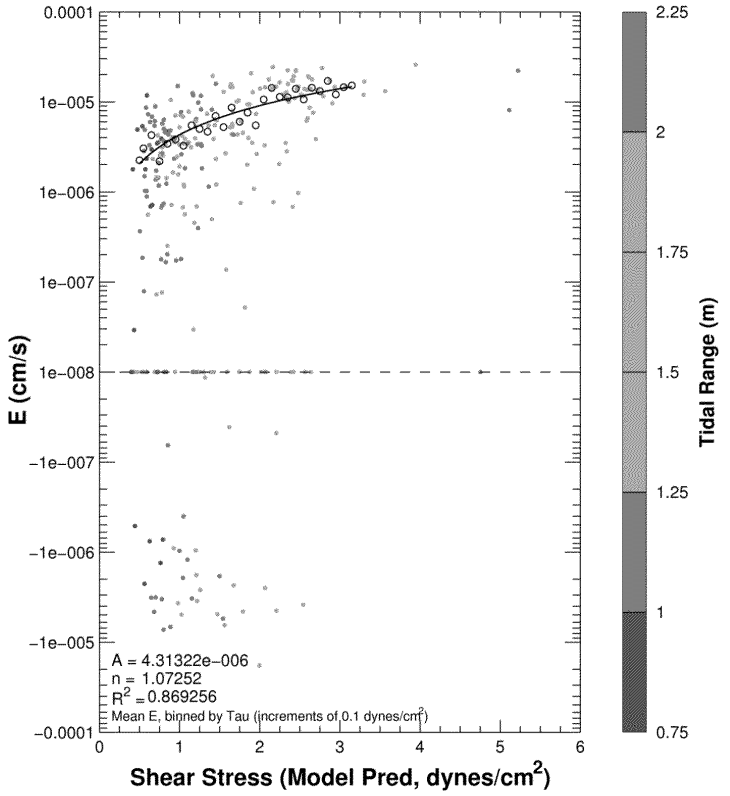

Figure 10. Calculated fluff layer entrainment rate versus shear stress. Binned values shown with hollow black circles.

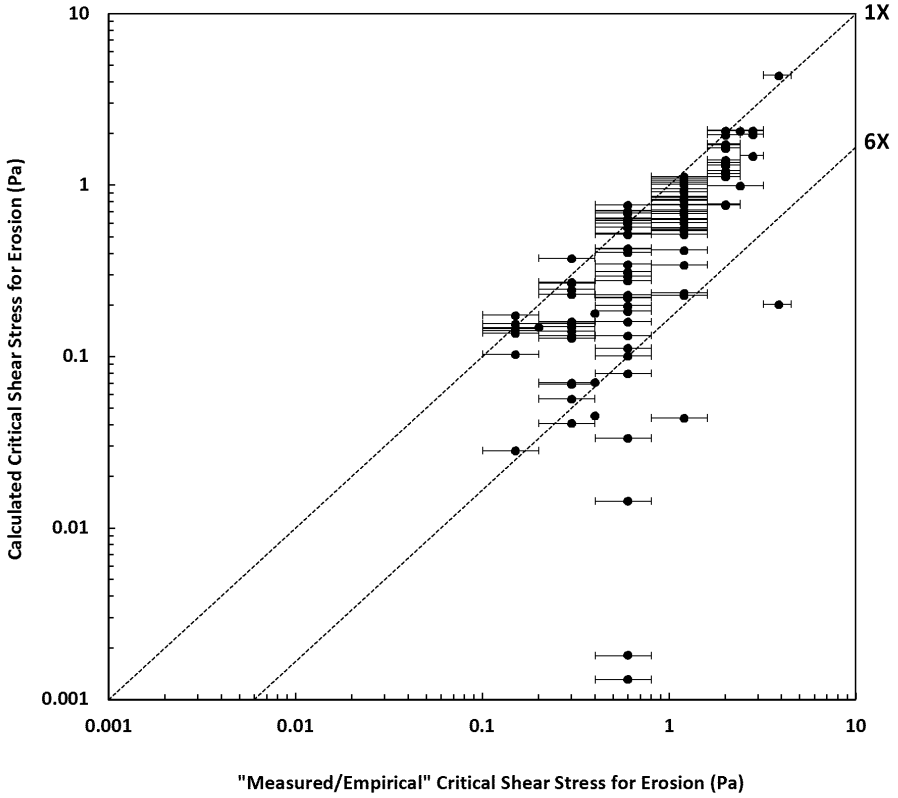

Figure 11. Calculated critical shear stress for erosion (corresponding to erosion rate of 10^{-4} cm/s) versus measured critical shear stress for erosion. Measured critical shear stress taken as the average of measured highest shear stress with no erosion and lowest shear stress with some erosion (range indicates the two values used in the computation of the average)

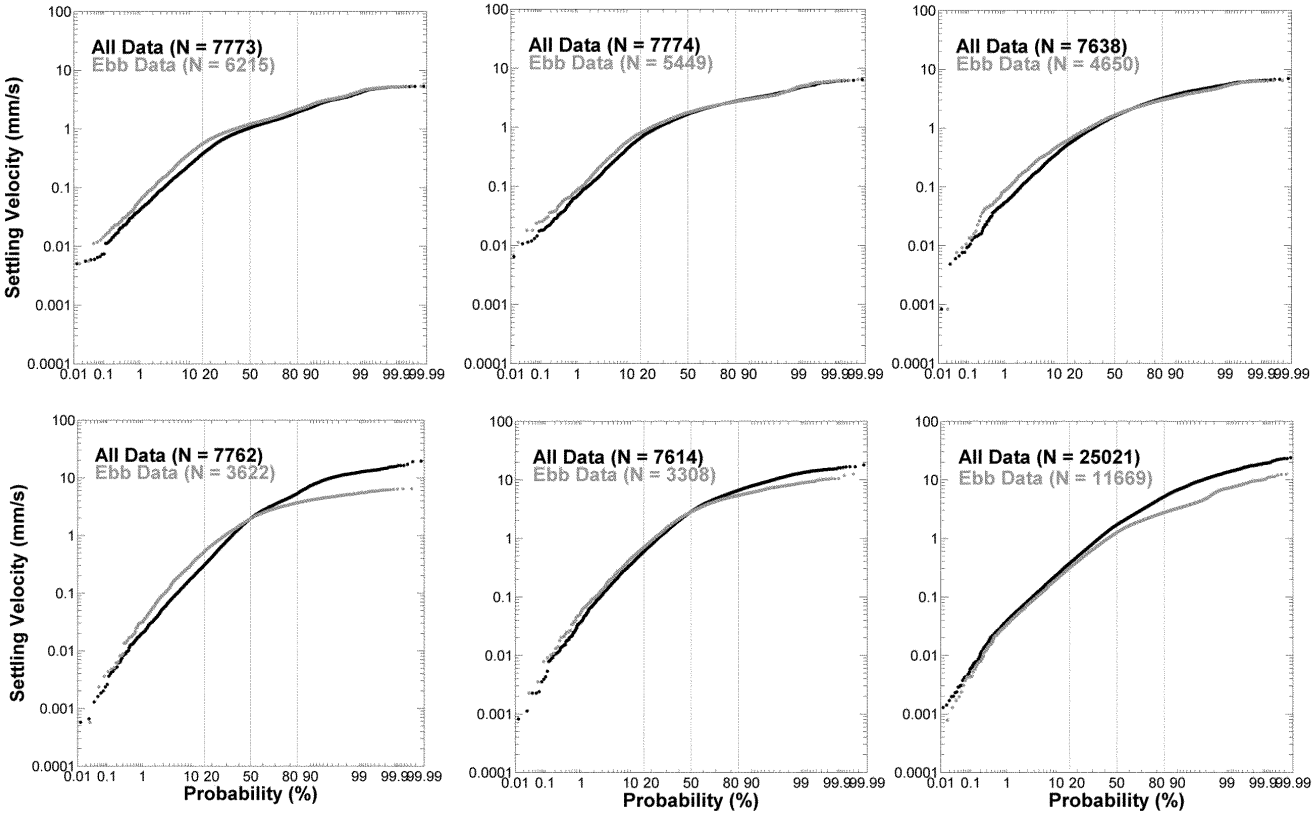

Figure 12. Distribution of calculated settling velocities from Fall 2009 PWCM data and Sommerfield and Chant (2010) data. Upper panels from left to right - RM 13.5, 10.2, and 6.7 from Fall 2009 PWCM. Lower panels from left to right - RM 4.2 and 1.4 from Fall 2009 PWCM, and RM 1.4 from Sommerfield and Chant (2010)

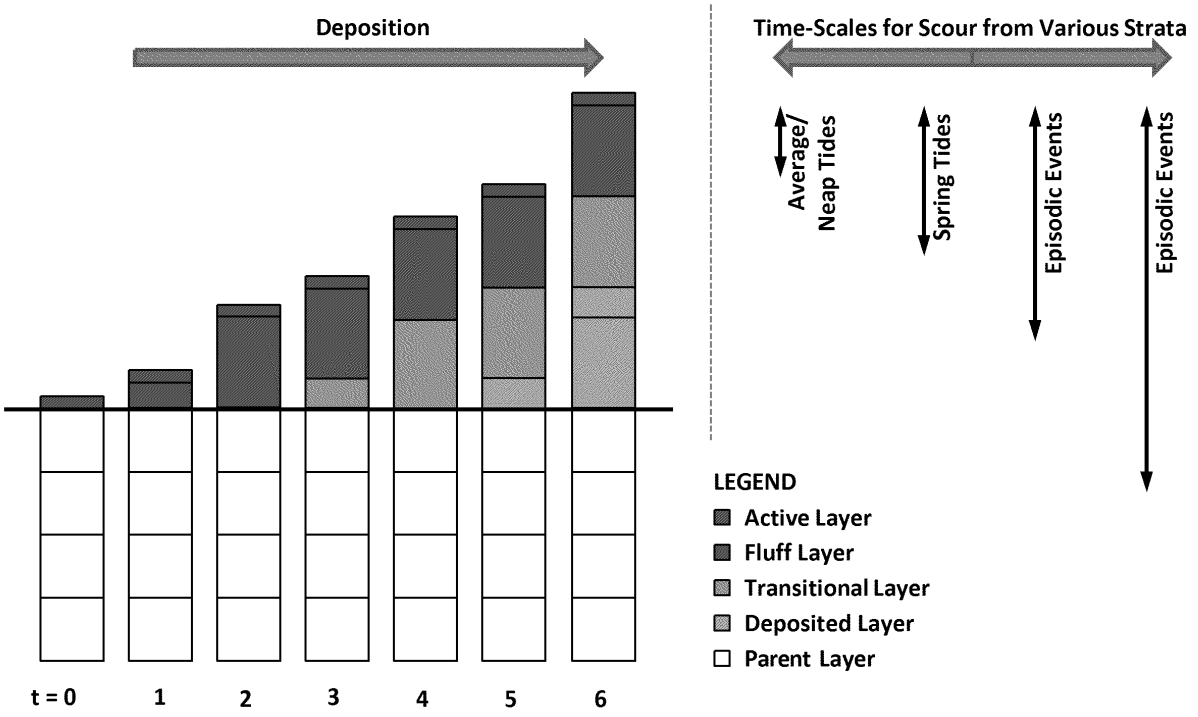

Figure 13. Schematic of revised bed layering in ECOM-SEDZLJS and conceptual representation of hydrodynamic conditions potentially responsible for erosion from various strata

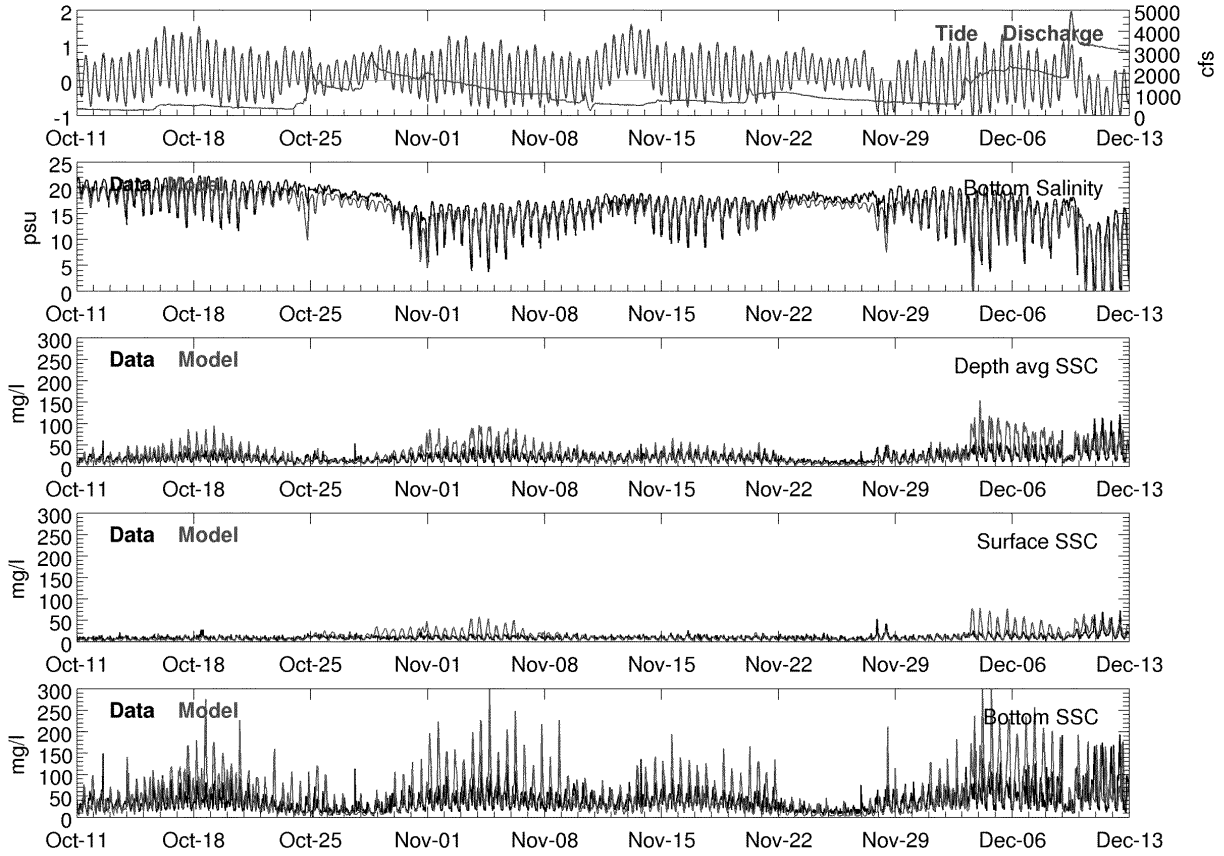

Figure 14. Time-series of model results and data during the Fall 2009 PWCM at RM 1.4

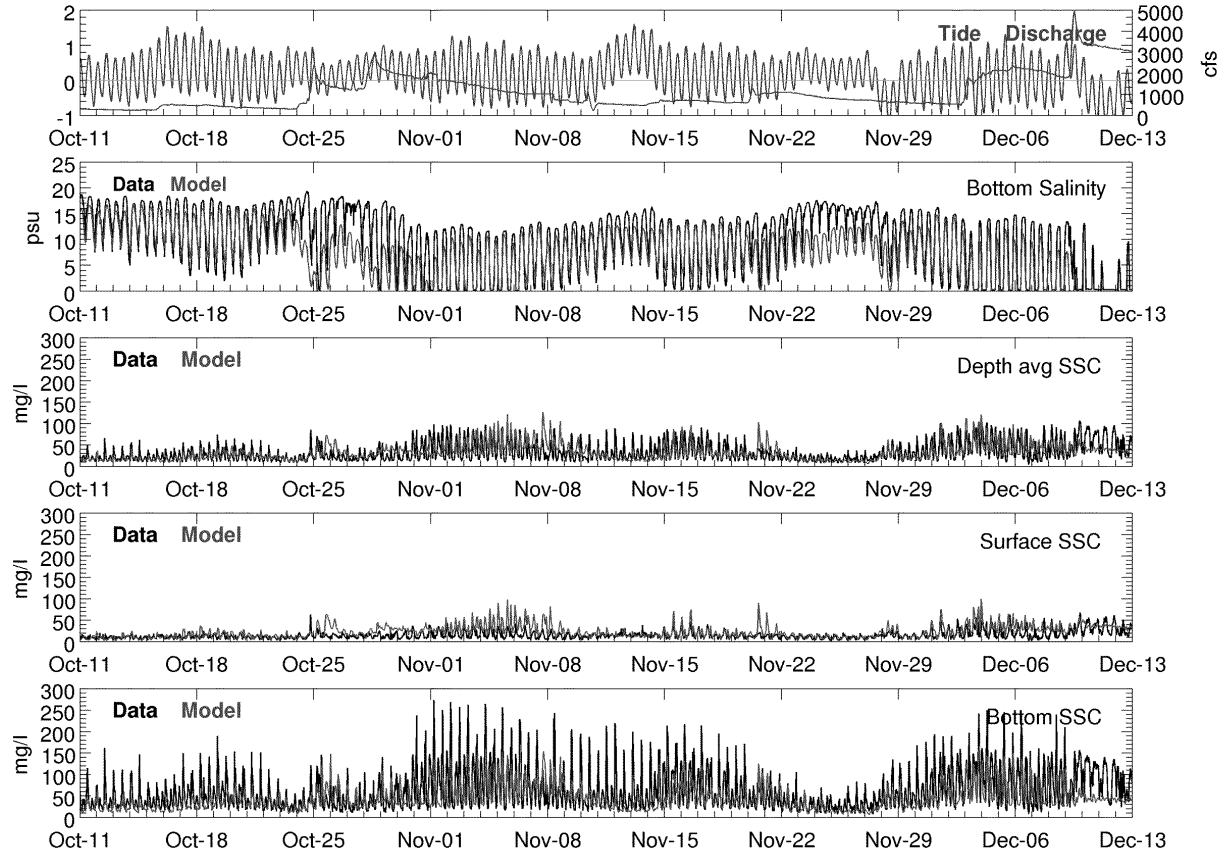

Figure 15. Time-series of model results and data during the Fall 2009 PWCM at RM 4.2

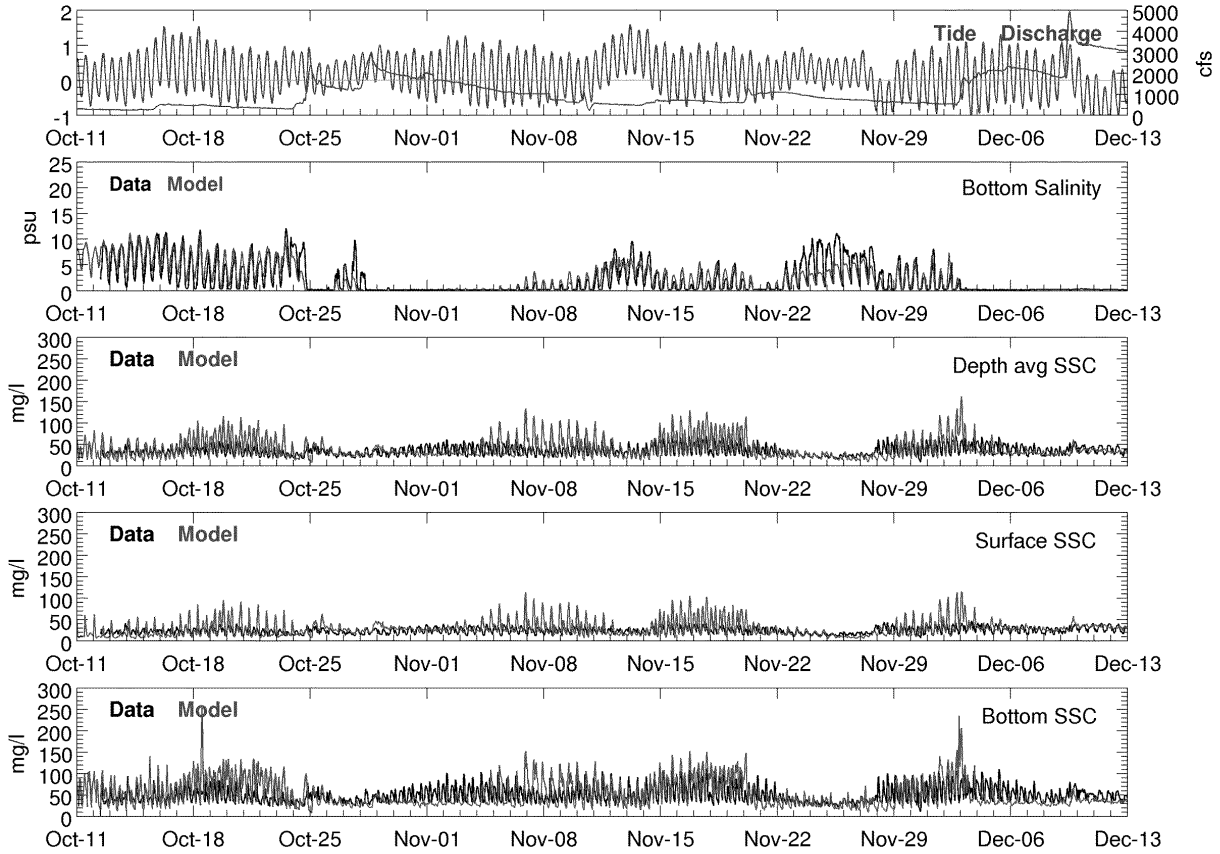

Figure 16. Time-series of model results and data during the Fall 2009 PWCM at RM 6.7

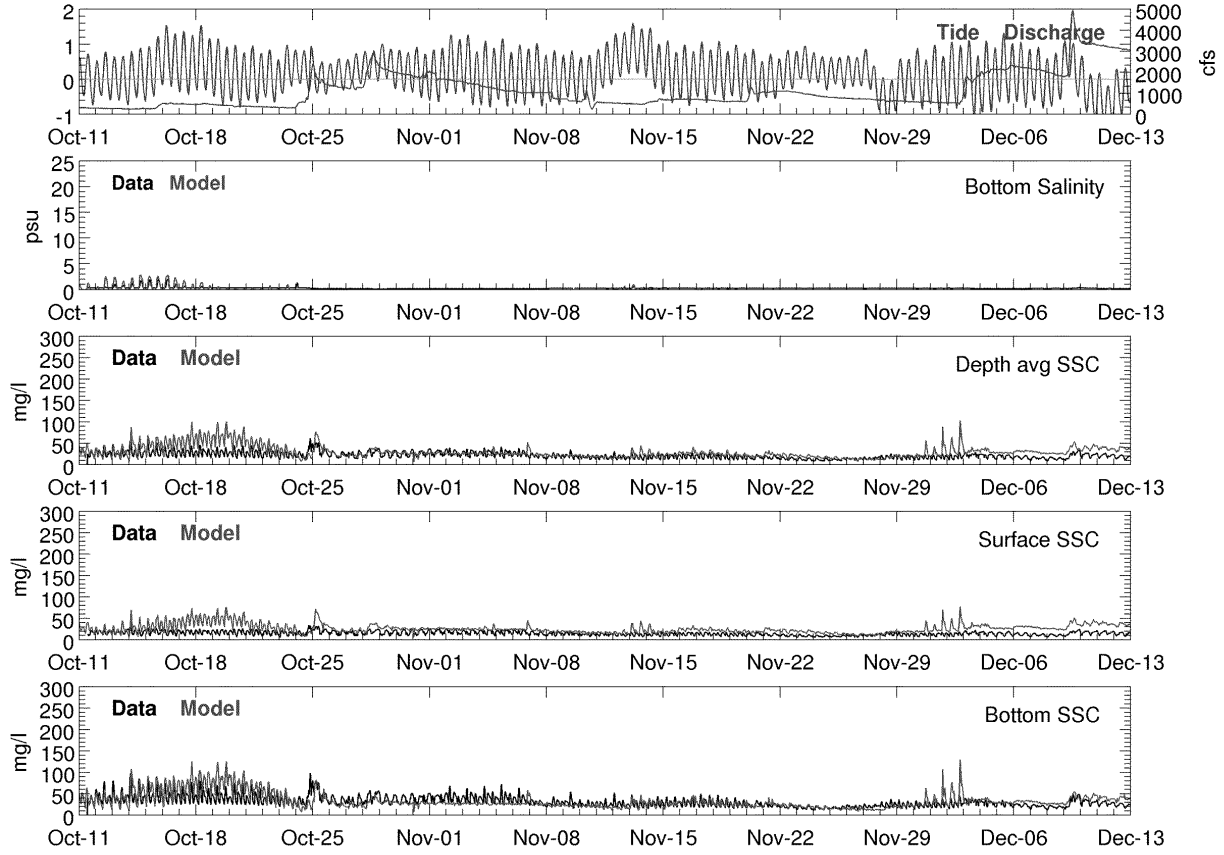

Figure 17. Time-series of model results and data during the Fall 2009 PWCM at RM 10.2

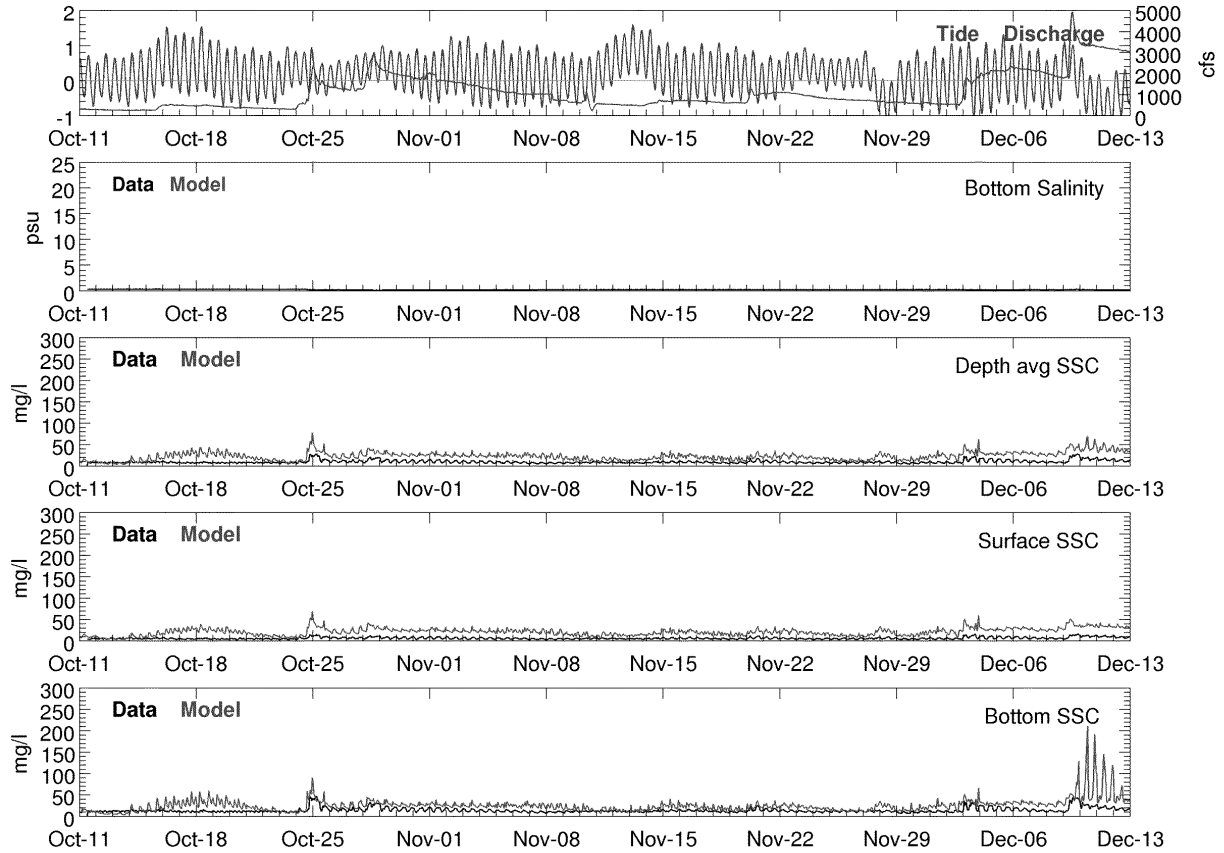

Figure 18. Time-series of model results and data during the Fall 2009 PWCM at RM 13.5

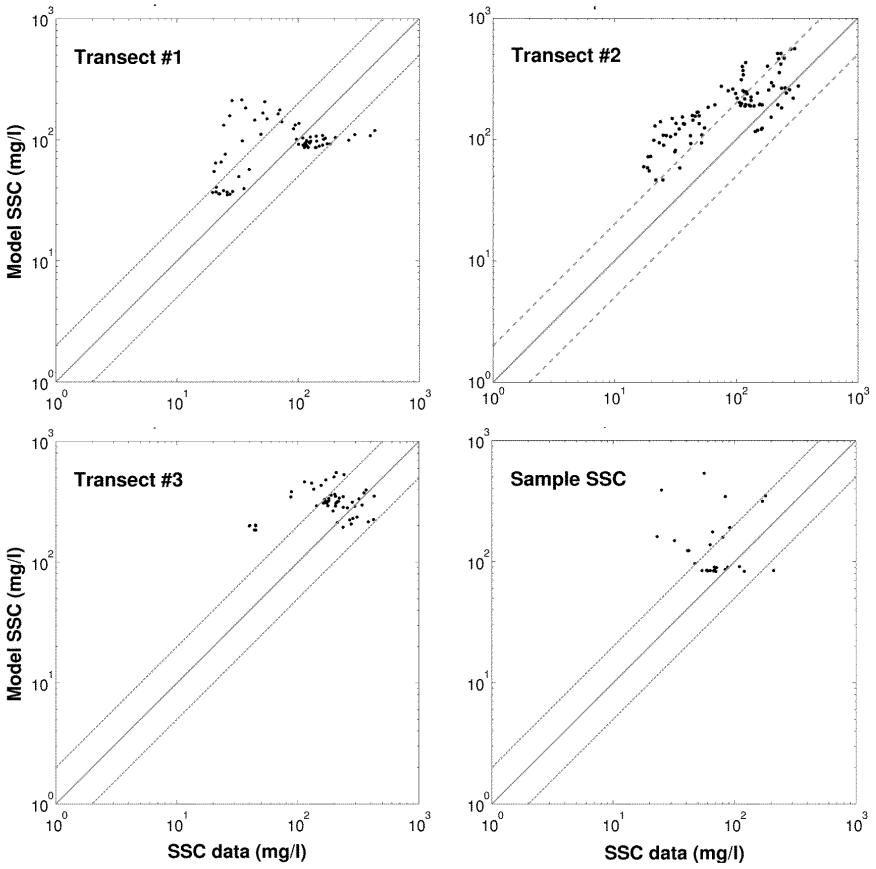

Figure 19. Model-data comparisons for high-flow event on March 16, 2010

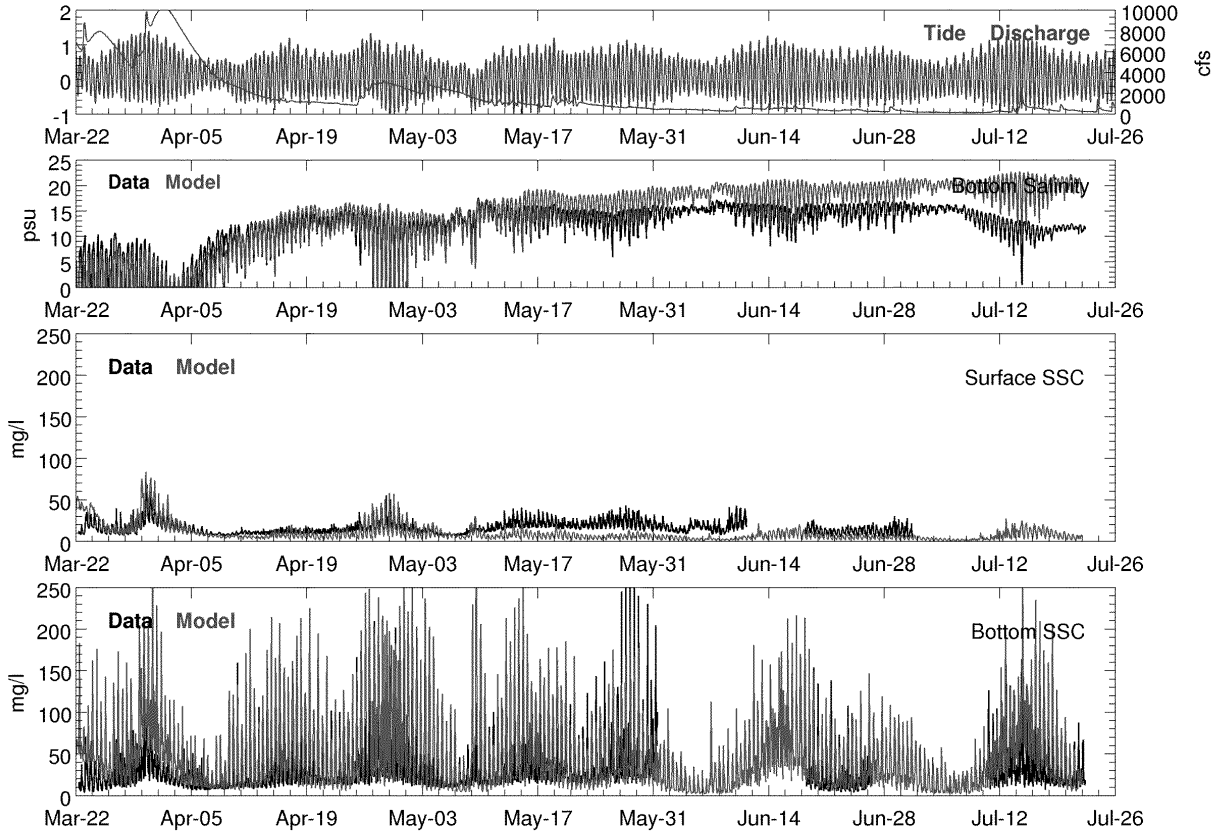

Figure 20. Time-series of model results and data during the Spring 2010 PWCM at RM 1.4

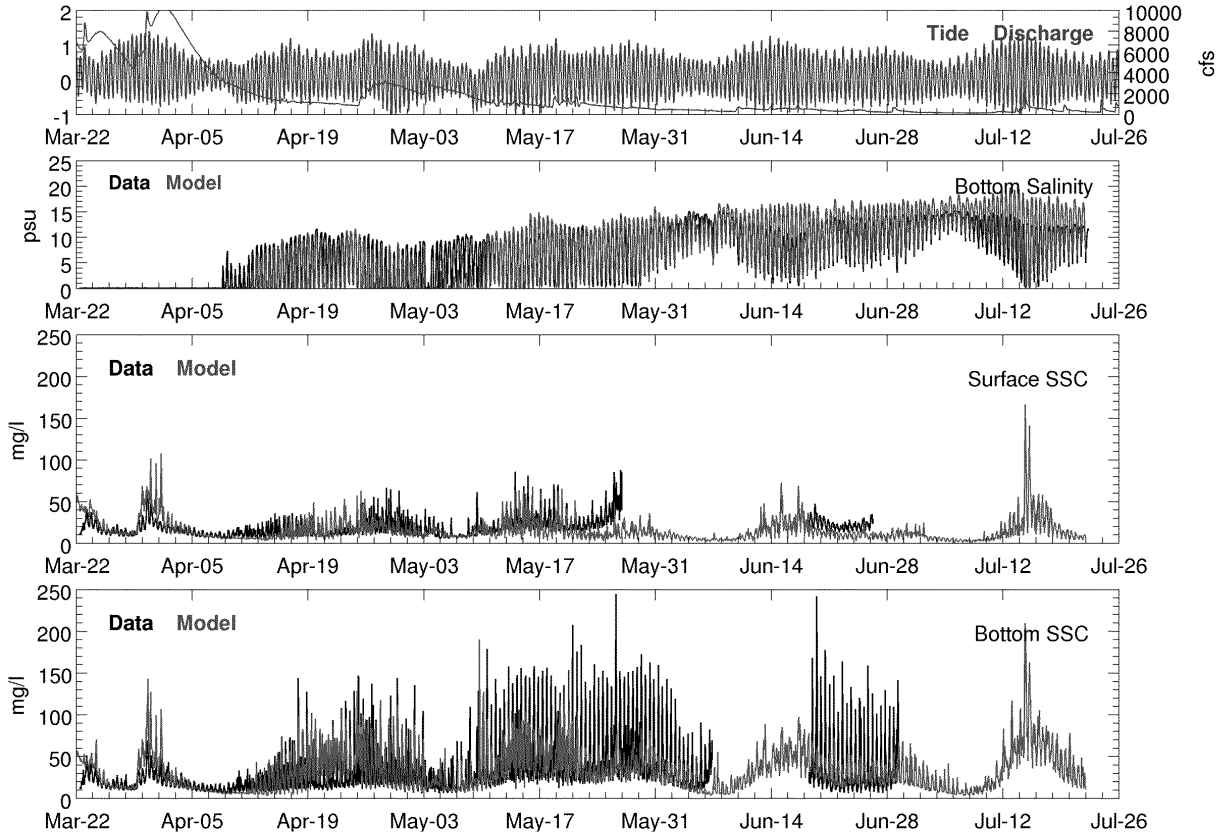

Figure 21. Time-series of model results and data during the Spring 2010 PWCM at RM 4.2

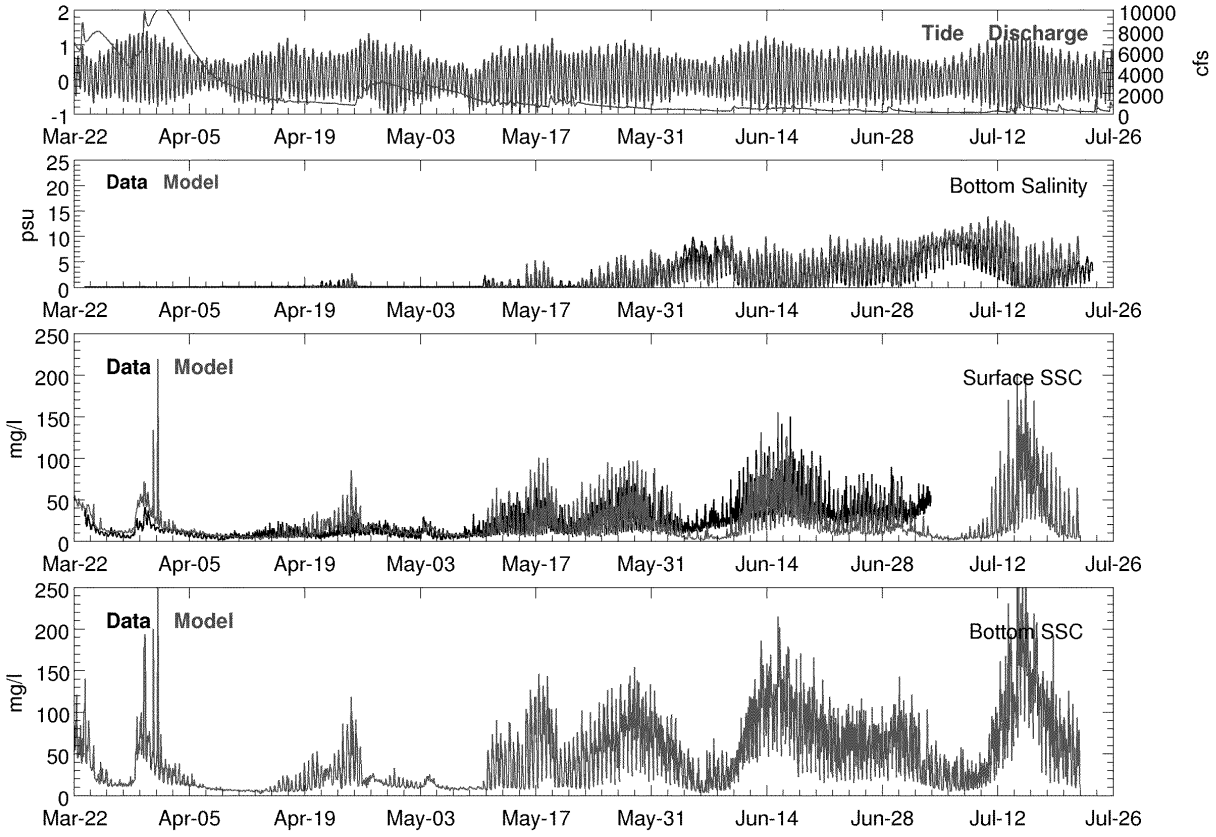

Figure 22. Time-series of model results and data during the Spring 2010 PWCM at RM 6.7

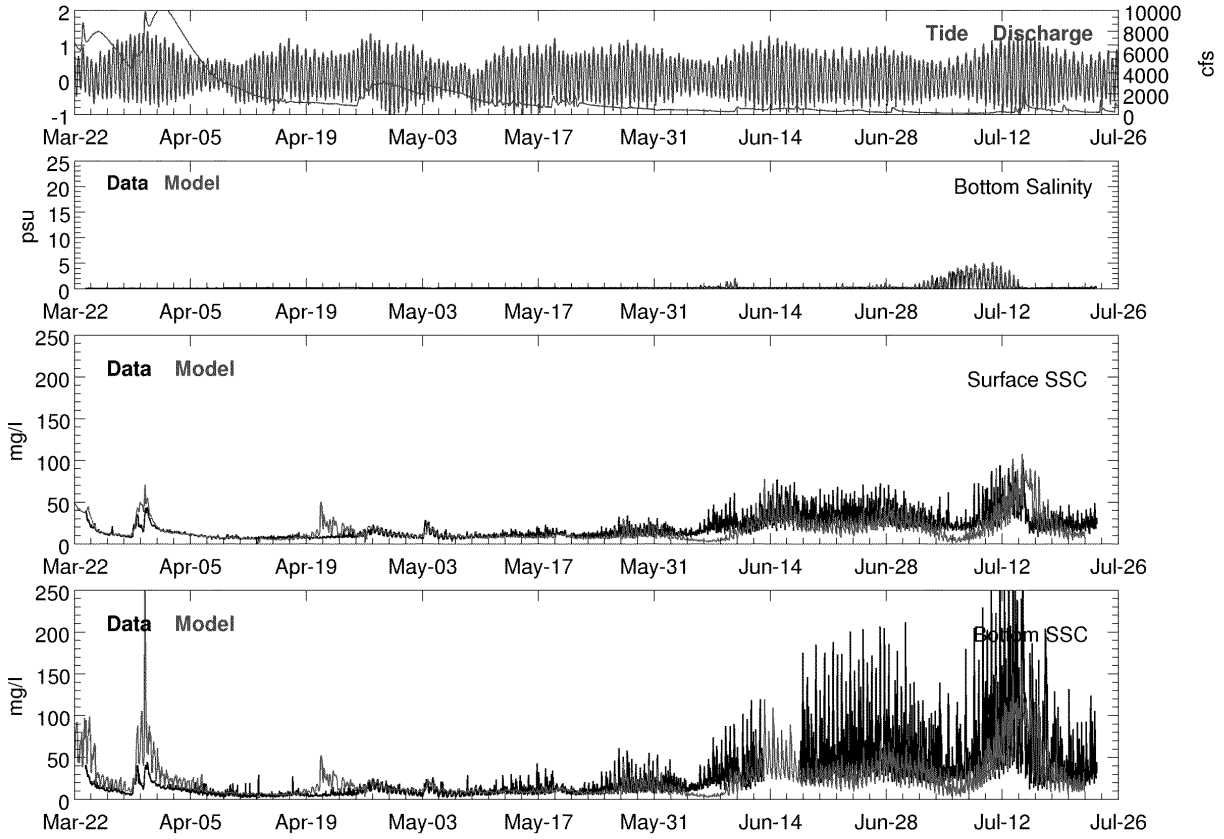

Figure 23. Time-series of model results and data during the Spring 2010 PWCM at RM 10.2

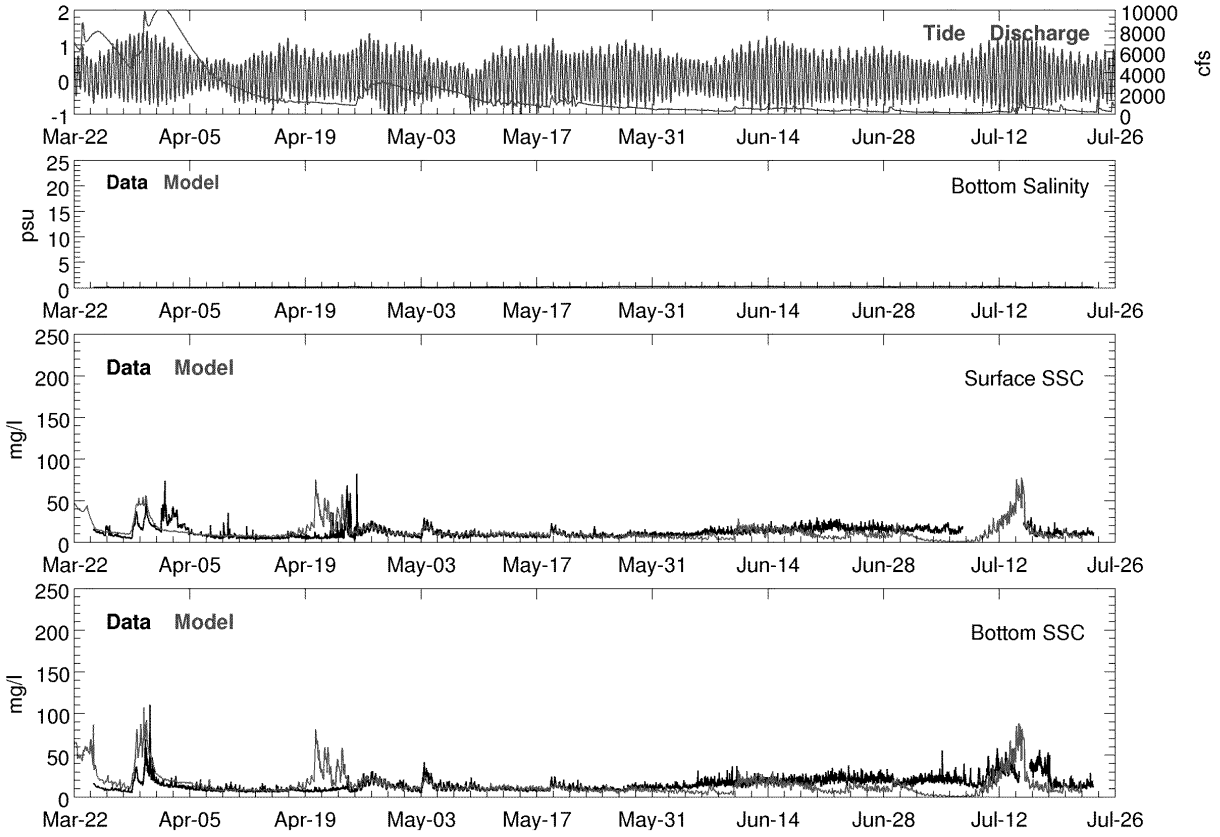

Figure 24. Time-series of model results and data during the Spring 2010 PWCM at RM 13.5

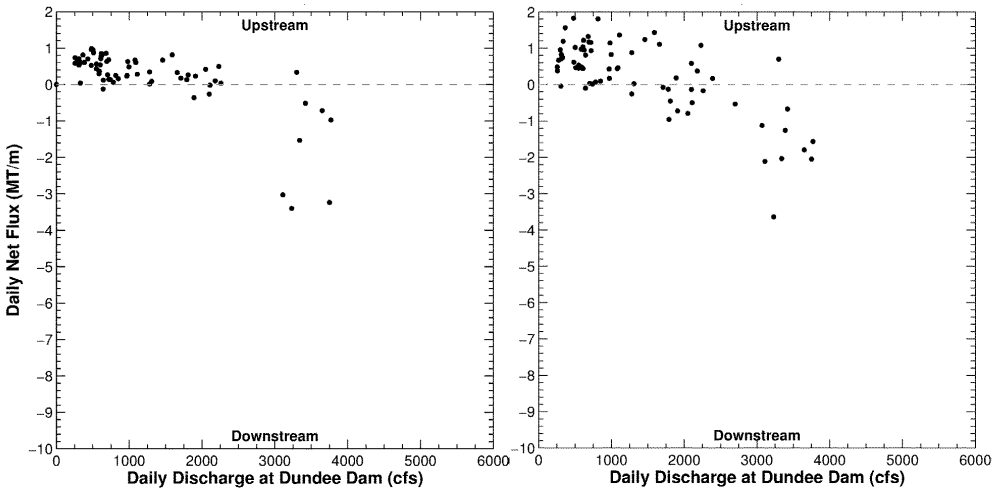

Figure 25. Sediment flux versus discharge during Fall PWCM from data (left) and model (right) at RM 1.4

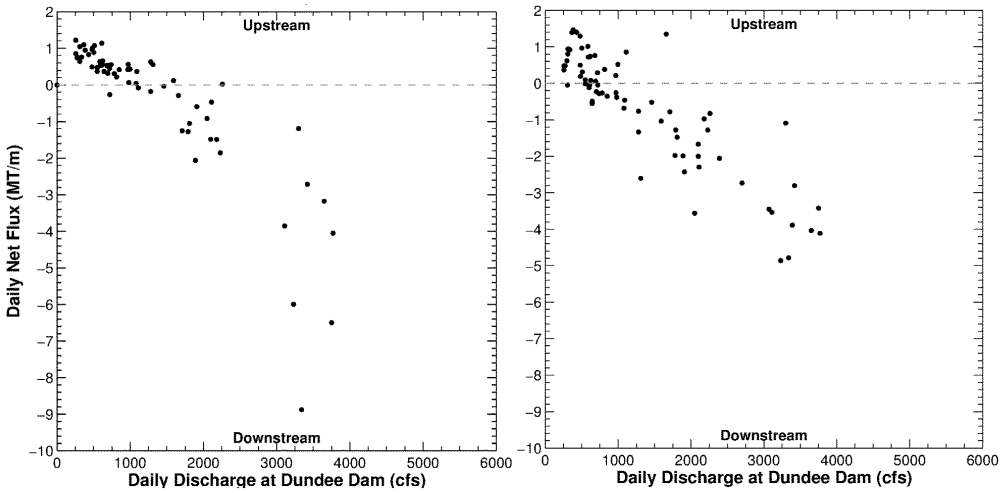

Figure 26. Sediment flux versus discharge during Fall PWCM from data (left) and model (right) at RM 4.2

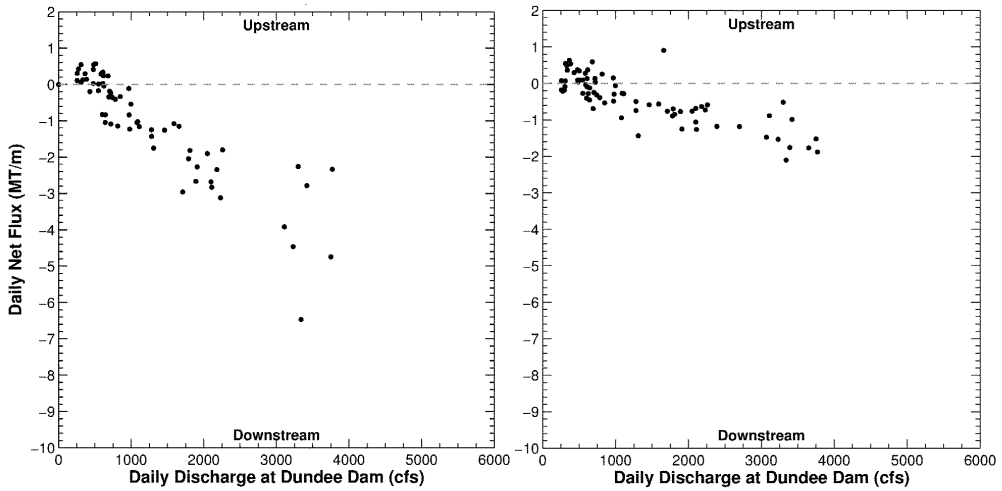

Figure 27. Sediment flux versus discharge during Fall PWCM from data (left) and model (right) at RM 6.7

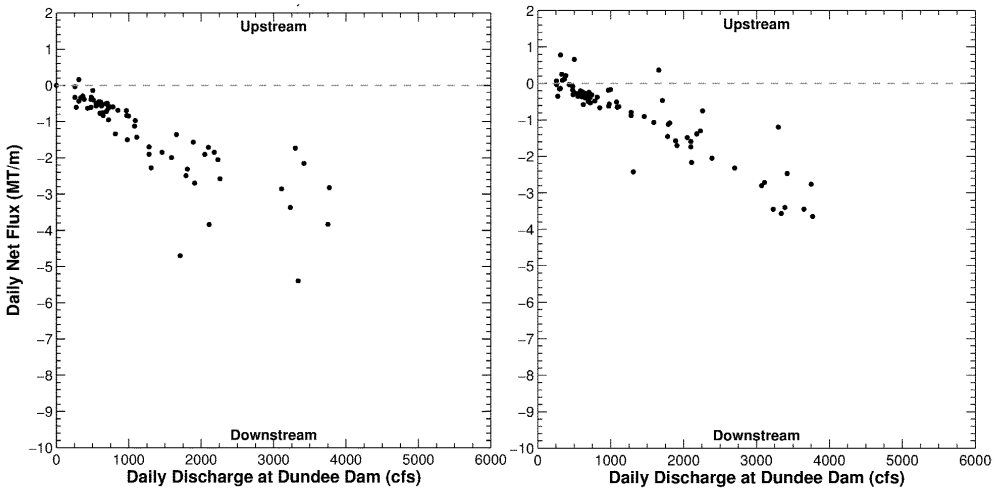

Figure 28. Sediment flux versus discharge during Fall PWCM from data (left) and model (right) at RM 10.2

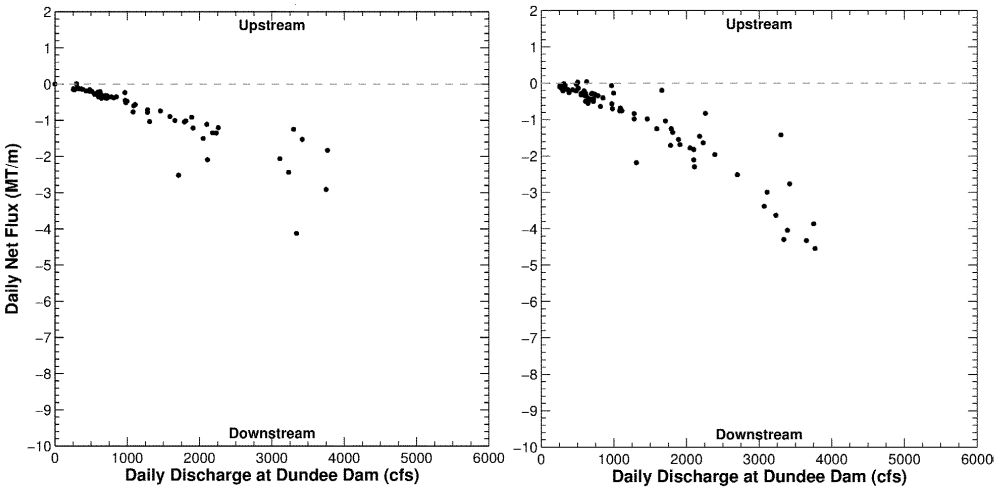

Figure 29. Sediment flux versus discharge during Fall PWCM from data (left) and model (right) at RM 13.5

Figure 30. Bathymetric change between the 2007-2008 multi-beam surveys. Data (left panel) and model (right panel)

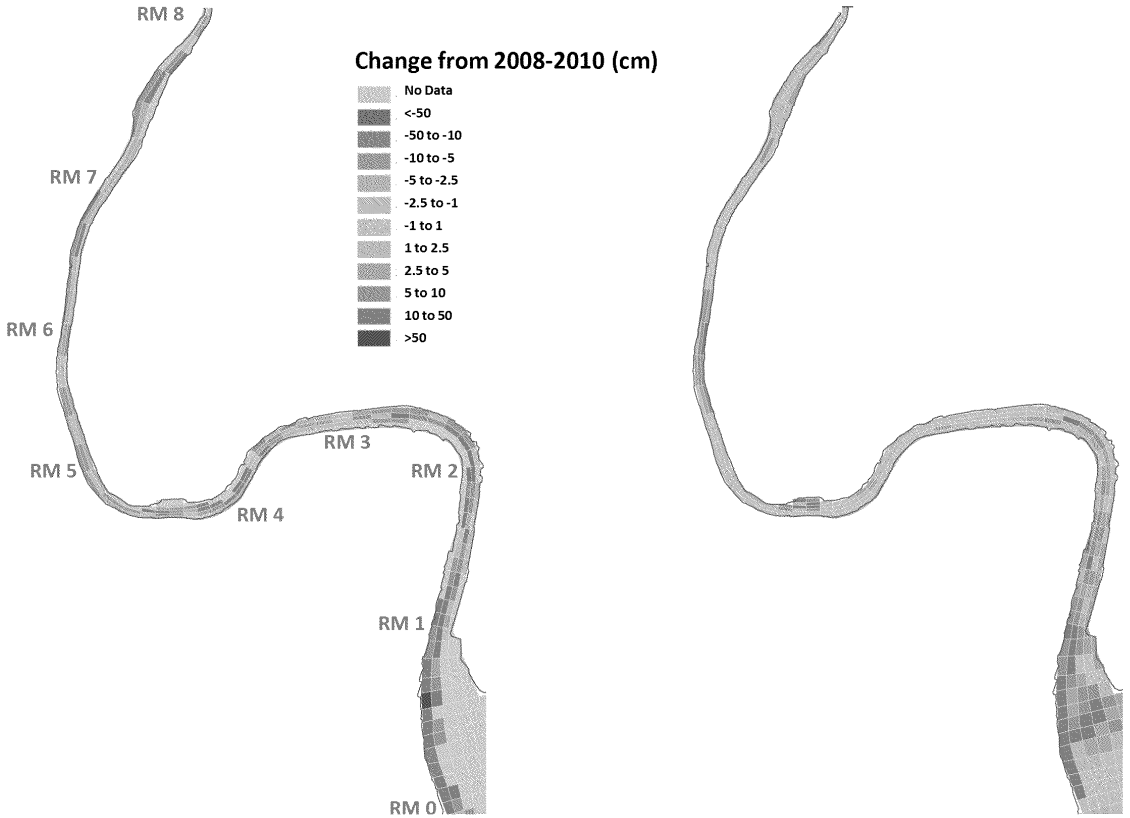

Figure 31. Bathymetric change between the 2008-2010 multi-beam surveys. Data (left panel) and model (right panel)

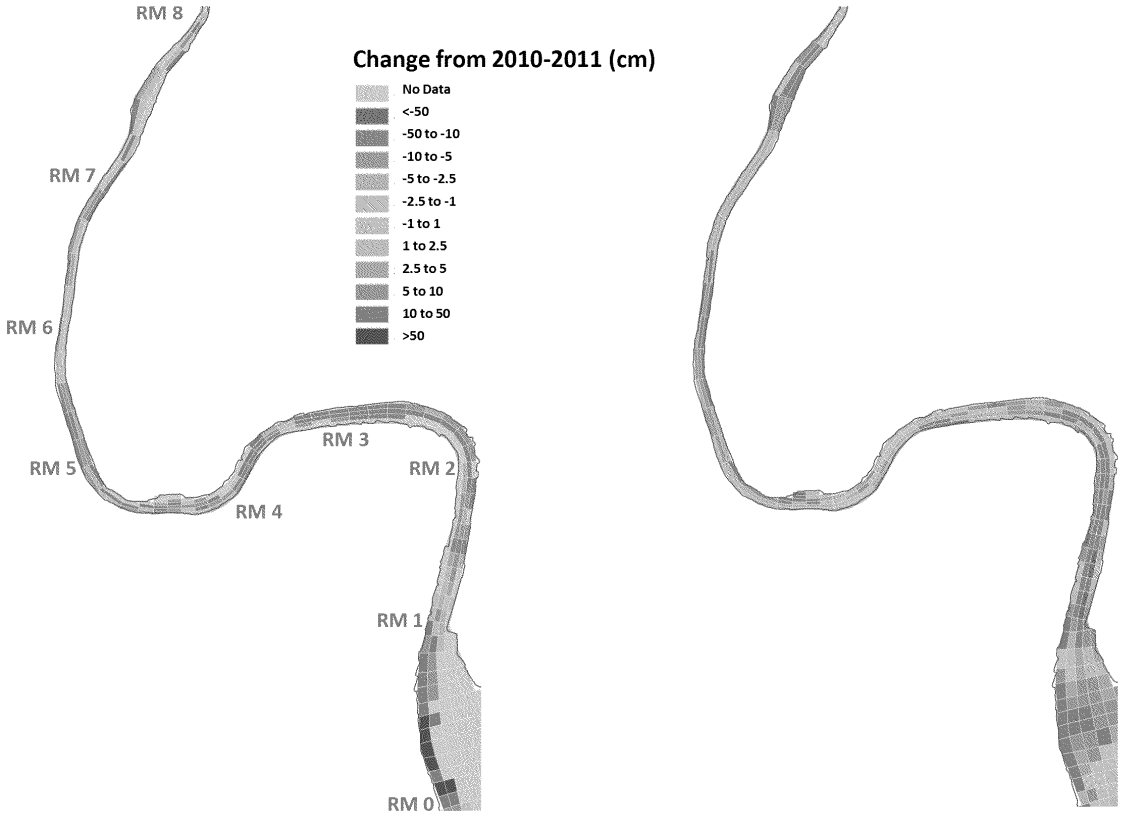

Figure 32. Bathymetric change between the 2010-2011 multi-beam surveys. Data (left panel) and model (right panel)

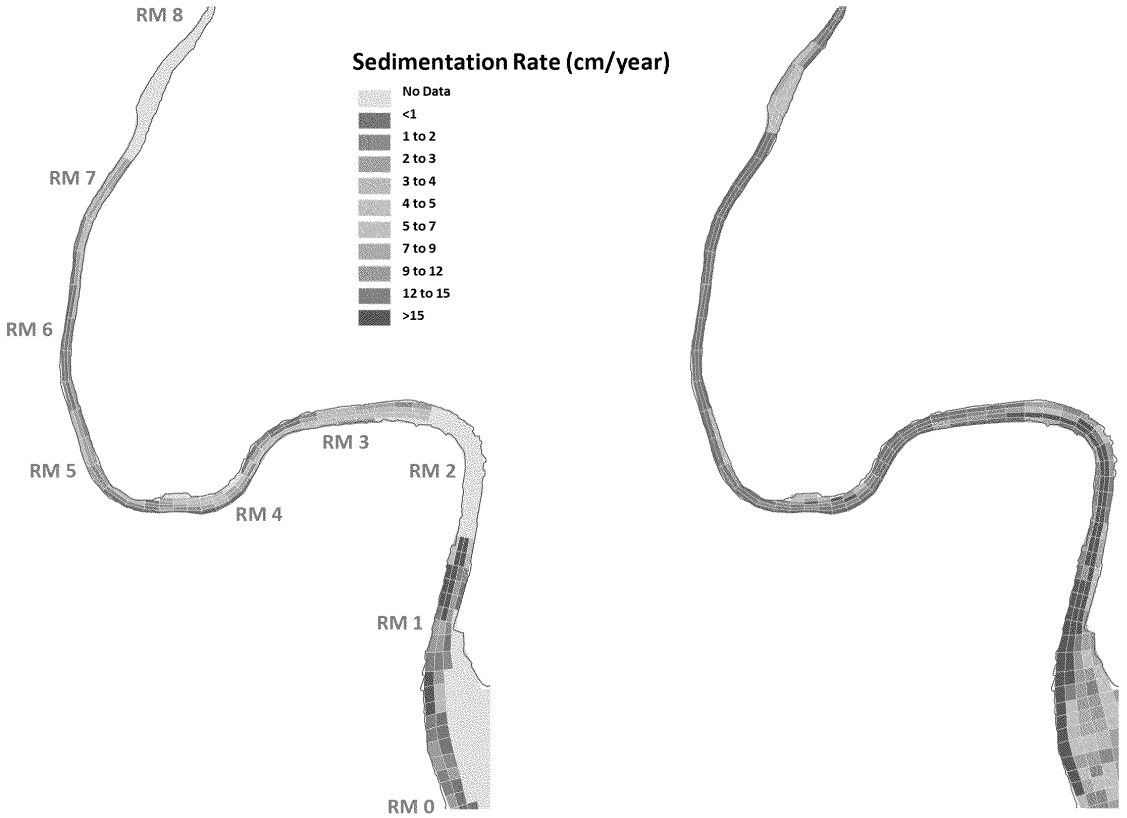

Figure 33. Infill rate under post-dredge conditions. Data (left panel; from 1949 to 2010 in RM 2-6.8, and from 1983 to 2010 in RM 0-1.5) and model (right panel; simulation using the WY1995-2010 boundary conditions with the design-depths for the navigation channel within the LPR)